

Cover Page



Universiteit Leiden



The handle <http://hdl.handle.net/1887/32582> holds various files of this Leiden University dissertation

**Author:** Wijngaarden, Marjolein A.

**Title:** Metabolic and endocrine adaptations to fasting in lean and obese individuals

**Issue Date:** 2015-03-26

# Chapter 5

## Regulation of skeletal muscle energy/nutrient-sensing pathways during metabolic adaptation to fasting in healthy humans

Marjolein A. Wijngaarden<sup>1\*</sup>, Leontine E.H. Bakker<sup>2\*</sup>, Gerard C. van der Zon<sup>3</sup>, Peter A.C. 't Hoen<sup>4</sup>, Ko Willems van Dijk<sup>1,5</sup>, Ingrid M. Jazet<sup>2</sup>, Hanno Pijl<sup>1</sup>, Bruno Guigas<sup>3,6</sup>

\* These authors contributed equally to this work

<sup>1</sup> Department of Endocrinology and Metabolism, Leiden University Medical Center, Leiden, The Netherlands

<sup>2</sup> Department of Internal Medicine, Leiden University Medical Center, Leiden, The Netherlands

<sup>3</sup> Department of Molecular Cell Biology, Leiden University Medical Center, Leiden, The Netherlands

<sup>4</sup> Center for Human and Clinical Genetics, Leiden University Medical Center, Leiden, The Netherlands

<sup>5</sup> Department of Human Genetics, Leiden University Medical Center, Leiden, The Netherlands

<sup>6</sup> Department of Parasitology, Leiden University Medical Center, Leiden, The Netherlands

*American Journal of Physiology – Endocrinology and Metabolism*  
2014;307(10):E885-95



## Abstract

During fasting, rapid metabolic adaptations are required to maintain energy homeostasis. This occurs by a coordinated regulation of energy/nutrient-sensing pathways leading to transcriptional activation and repression of specific sets of genes. The aim of the study was to investigate how short-term fasting affects whole-body energy homeostasis and skeletal muscle energy/nutrient-sensing pathways and transcriptome in humans. For this purpose, twelve young healthy men were studied during a 24-hour fast. Whole-body glucose/lipid oxidation rates were determined by indirect calorimetry and blood and skeletal muscle biopsies were collected and analyzed at baseline and after 10 and 24h of fasting. As expected, fasting induced a time-dependent decrease in plasma insulin and leptin levels, whereas levels of ketone bodies and free fatty acids increased. This was associated with a metabolic shift from glucose towards lipid oxidation. At the molecular level, activation of the protein kinase B (PKB/Akt) and mammalian target of rapamycin (mTOR) pathways was time-dependently reduced in skeletal muscle during fasting, whereas the AMP-activated protein kinase (AMPK) activity remained unaffected. Furthermore, we report some changes in the phosphorylation and/or content of forkhead protein 1 (FoxO1), sirtuins 1 (SIRT1) and class IIa histone deacetylase 4 (HDAC4), suggesting that these pathways might be involved in the transcriptional adaptation to fasting. Finally, transcriptome profiling identified genes that were significantly regulated by fasting in skeletal muscle at both early and late time-points. Collectively, our study provides a comprehensive map of the main energy/nutrient-sensing pathways and transcriptomic changes during short-term adaptation to fasting in human skeletal muscle.

## Introduction

During evolution, an integrated system regulating substrate storage and utilization at the whole organism level has developed by means of nutrient and energy sensors that constantly gauge the change in metabolic or environmental conditions. One example is the decrease in glycogen storage observed during fasting, which is associated with a concomitant shift in substrate utilization from carbohydrate to lipid oxidation, aiming to preserve glucose for use by the brain and maintain whole-body energy homeostasis <sup>1</sup>.

As a metabolically flexible tissue, skeletal muscle contributes to a large extent to this whole-body metabolic adaptation that occurs through complex and coordinated regulation of several energy/nutrient-sensing pathways <sup>2</sup>. Among them, the serine/threonine AMP-activated protein kinase (AMPK) is considered one of the main sensors of energy depletion. Once activated, AMPK acts to restore energy balance by switching off energy-consuming pathways and promoting ATP-generating processes <sup>3-5</sup>. AMPK consists of a heterotrimeric complex containing a catalytic subunit  $\alpha$  and two regulatory  $\beta$  and  $\gamma$  subunits. Phosphorylation of the  $\alpha$  subunit at Thr172 by upstream AMPK kinases (AMPKKs), such as the liver kinase B (LKB1) or calmodulin-dependent protein kinase kinase  $\beta$  (CAMKK $\beta$ ), is required for AMPK activation. The  $\beta$  subunit acts as a scaffold to which the two other subunits are bound, and contains a carbohydrate binding site which allows AMPK to sense energy reserves in the form of glycogen <sup>3-5</sup>. When cellular energy status is threatened, the binding of AMP and/or ADP to the  $\gamma$  subunit activates AMPK via a complex mechanism involving direct allosteric activation, phosphorylation on Thr172 by AMPKKs, and inhibition of dephosphorylation by protein phosphatase(s) <sup>3-5</sup>. Interestingly, animal studies suggest that skeletal muscle AMPK activation rapidly occurs during fasting <sup>6</sup>, triggering the transcriptional modulation of genes involved in lipid and glucose metabolism <sup>7</sup>.

Other energy/nutrient-sensing pathways, such as the mammalian target of rapamycin (mTOR) <sup>8</sup>, some forkhead protein (FoxO) family members <sup>9,10</sup>, sirtuins 1 (SIRT1) <sup>11</sup> and the class IIa histone deacetylase 4 (HDAC4) <sup>12</sup>, were also suggested to be involved in the metabolic shift towards lipid oxidation during fasting in peripheral tissues. Interestingly, all these pathways are tightly interconnected with AMPK <sup>13-15</sup>, suggesting that the kinase could play a central role in skeletal muscle metabolic flexibility.

Modulation of energy/nutrient-sensing pathways are likely to be involved in health

and diseases. Indeed, calorie restriction was shown to extend lifespan and delay the onset of age-related diseases in a wide spectrum of organisms <sup>16</sup>, partly by inducing acute and long-lasting changes in energy/nutrient-sensing signaling pathways <sup>17-20</sup>. A better understanding of the energy/nutrient-sensing machinery in humans would therefore provide important insight into the pathophysiology of various age-related diseases, including type 2 diabetes and cancer. To the best of our knowledge, there is currently no data available reporting the kinetic of response of energy/nutrient-sensing pathways in human skeletal muscle during fasting. The purpose of the present study was therefore to investigate how short-term fasting affects whole-body energy homeostasis and skeletal muscle energy/nutrient-sensing pathways and transcriptome in healthy humans.

---

## Methods

### *Ethical approval*

The present study (Clinical Trial Registration Number: NCT01387919) was approved by the Medical Ethical Committee of the Leiden University Medical Center and performed in accordance with the principles of the revised Declaration of Helsinki. All volunteers gave written informed consent before participation.

### *Subjects*

Twelve lean male volunteers (body mass index (BMI)  $21.3 \pm 0.6$  kg/m<sup>2</sup>, age  $22 \pm 1$  year-old) were included. All of them were healthy weight-stable non-smoking Caucasians with a fasting plasma glucose  $\leq 5.6$  mmol/l and without family history of diabetes. Height, weight and body mass index (BMI) were measured according to World Health Organization recommendations.

### *Study design*

All participants were instructed not to perform physical activity in the last 48 hours before the study day and were admitted to our research center after an overnight fast. The intervention study started after a standardized breakfast (t=0, two slices of brown bread with cheese; 300 calories), followed by 24 hours of fasting. Water and caffeine-free tea were allowed *ad libitum*. Blood samples were taken after breakfast (t=90 min), and after 10 and 24 hours of fasting by the means of an intravenous cannula, which was inserted in the elbow just before breakfast. Muscle biopsies from *musculus vastus lateralis* were collected after breakfast (baseline, t=105 min), and after 10 and 24 hours of fasting under localized 1% lidocain anesthesia, as previously described<sup>21</sup>.

### *Indirect calorimetry*

Subjects were placed under the ventilated hood after ~75 min, 10 and 24 hours of fasting (OxyconPro, Mijnhardt Jaegher, The Netherlands). Respiratory quotient and substrate oxidation were calculated from CO<sub>2</sub> and O<sub>2</sub> concentrations in the exhaled air, as previously described<sup>22</sup>.

### *Laboratory analysis*

Serum glucose, total cholesterol, triglycerides (TG), free fatty acids (FFA), alkaline

---

phosphatase and creatinine were measured on a Modular Analytics P-800 system (Roche Diagnostics, Germany). Serum insulin and insulin-like growth factor 1 (IGF-1) were measured by immunoluminometric assay on an Immulite 2500 automated system (Siemens Healthcare Diagnostics, The Netherlands). Cortisol, free T4 (FT4) and thyroid stimulating hormone (TSH) were measured by electrochemoluminescence immunoassay on a Modular Analytics E-170 system (Roche Diagnostics, Germany). Triiodothyronine (T3) was measured with by fluorescence polarization immunoassay on an AxSym system (Abbott, US). Growth hormone (GH) was measured by immunofluorometric assay (Wallac, Finland). Serum active ghrelin, leptin and adiponectin were determined by radioimmunoassay (Millipore, USA). Testosterone was determined by a direct RIA of Siemens Healthcare Diagnostics, Sex hormone-binding globulin (SHBG) was measured on an automated Immulite 2500 (Siemens, Breda, The Netherlands). Ketone bodies were measured using test strips on the Precision Xtra™ Blood Glucose and Ketone Monitoring System (Abbott, North Chicago, Illinois)

#### *Western Blot*

Skeletal muscle biopsies (~30-45 mg) were homogenized by Ultra-Turrax (22 000 rpm; 2x5 sec) in a 6:1 (v/w) ratio of ice-cold buffer containing: 50 mM HEPES (pH 7.6), 50 mM NaF, 50 mM KCl, 5 mM NaPPi, 1 mM EDTA, 1 mM EGTA, 5 mM  $\beta$ -GP, 1 mM Na<sub>3</sub>VO<sub>4</sub>, 1 mM DTT, 1% NP40 and protease inhibitors cocktail (Complete, Roche, The Netherlands). Western blots were performed using phospho-specific (Ser473-PKB, phospho-Akt substrate, Ser2448-mTOR, Ser235/236-S6, Thr172-AMPK $\alpha$ , Ser221-ACC, Ser498-HDAC4, Ser47-SIRT1 and Thr24-FoxO1 from Cell Signaling) or total primary antibodies (Tubulin, AMPK $\alpha$ , ACC and FoxO1 from Cell Signaling; HDAC4, SIRT1 and MitoProfile OXPHOS from AbCam; IR $\beta$  from Santa Cruz; NAMPT from Bethyl Laboratories), as previously described<sup>23</sup>.

#### *AMPK activity*

AMPK heterotrimeric complexes were immunoprecipitated from 500  $\mu$ g of muscle lysate using protein A-agarose beads (GE Healthcare, The Netherlands) and a pan  $\alpha$ -specific AMPK antibody (Santa Cruz) incubated together at 4°C overnight on a rotating wheel. The AMPK activity was measured in the immunoprecipitate by radioactive assay using [ $\gamma$ -<sup>32</sup>P]ATP, as previously described<sup>24</sup>.



---

### *RNA isolation*

Total RNA was isolated from skeletal muscle biopsies (~25-30 mg) using the phenol-chloroform extraction method (Tripure RNA Isolation reagent, Roche, Germany), treated with the TurboDNase kit according to manufacturer protocol (TurboDNase, Life Technologies, The Netherlands) and quantified by NanoDrop (ND1000, Thermo Scientific, The Netherlands). The quality and integrity of RNA was tested using 2100 Bioanalyzer (Agilent Technologies, Waldbronn, Germany) and all the samples had a RNA integrity number score >8.

### *Microarray and real-time RT-PCR*

For microarray analysis, Illumina TotalPrep-96 RNA Amplification kit was used to generate biotin labeled, amplified cRNA starting from 200ng total RNA. 750 ng of the obtained biotinylated cRNA samples was hybridized onto the Illumina HumanHT-12 v4 BeadChip array. Primary gene expression analysis of the scanned BeadChip arrays was performed using Illumina's Genomestudio v.2011.1. Analysis was performed with the lumi package version 2.4.0 in R<sup>25</sup>. Data was subjected to a *variance stabilizing transformation (VST function)*, and subjected to quantile normalization. The difference relative to the post-meal (baseline) condition was calculated from the mean normalized intensities for each condition, assuming a log<sub>2</sub> scale, and fold-change were calculated after back-transformation to the linear scale. The significance of difference in gene expression relative to the post-meal condition was calculated from a hierarchical linear model, as implemented in the limma package version 3.8.3, with expression as dependent variable and time point and individual as categorical, independent variables. The fold change *versus* post-meal condition was calculated as the absolute ratio of normalized intensities between the mean values of all individual fold changes (post-meal/10h or 24h fasting). Two cutoff values were used to select the regulated genes and minimize the chances of false positives: fold changes >1.25 and p≤0.05 (up-regulated) and fold changes <0.75 and p≤0.05 (down-regulated). The gene lists of interest were next generated and analyzed for enriched gene ontology (GO) terms for biological processes, molecular functions, protein classes and pathways using the Web-based software PANTHER 8.1<sup>26</sup>. The microarray data have been deposited in the NCBI Gene Expression Omnibus (GEO) repository under no. GSE55924. For real-time RT-PCR, first-strand cDNA was synthesized from 1 µg total RNA using a Superscript first strand synthesis kit (Invitrogen, The Netherlands). Real-time PCR assays were performed using specific primers sets (sequences provided on request)

---

and SYBR Green on a StepOne Plus Real-time PCR system (Applied Biosystems, US). mRNA expression was normalized to ribosomal protein S18 (*Rps18*) and expressed as mean log<sub>2</sub> change *versus* post-meal group.

*Statistical analysis*

All data are presented as mean ± standard error of the mean (SEM). A mixed model was used to compare all measurements during fasting with the baseline (post-meal) values: time was modeled as fixed effect while random intercepts were used to model the subject-specific deviation from the mean. Within each analysis, a Bonferroni post hoc test was used to adjust for multiple comparisons. All the statistical analysis were performed using SPSS 18.0 for Windows (SPSS Inc., US).

## Results

### *Effects of fasting on body weight and metabolic parameters*

The anthropometric and metabolic characteristics of the subjects were determined at baseline (post-meal, ~90 min after a standardized breakfast of 300 Kcal), and after 10 and 24 hours of fasting (Table 1). Body weight decreased upon fasting (-1.9%;  $p < 0.05$ ). As expected, a significant time-dependent decrease in plasma insulin, leptin

**Table 1. Anthropometric and metabolic parameters at baseline and during fasting**

	Post-meal	10h fast	24h fast
<b>Age (years)</b>	22 ± 1		
<b>Length (cm)</b>	184 ± 1		
<b>Weight (kg)</b>	72 ± 2	nd	71 ± 2*
<b>Body mass index (kg/m<sup>2</sup>)</b>	21.3 ± 0.6	nd	20.9 ± 0.5*
<b>Glucose (mmol/l)</b>	4.0 ± 0.1	4.2 ± 0.1	3.8 ± 0.1
<b>Insulin (mU/l)</b>	3.8 ± 1.0	1.0 ± 0.2*	1.0 ± 0.2*
<b>Growth Hormone (mU/l)</b>	0.3 ± 0.1	2.8 ± 0.9	4.8 ± 2.2*
<b>IGF-1 (nmol/l)</b>	24.9 ± 1.9	25.8 ± 2.3	26.4 ± 2.3
<b>Leptin (µg/l)</b>	1.4 ± 0.4	1.0 ± 0.3	0.5 ± 0.2*
<b>Adiponectin (µg/l)</b>	7.4 ± 0.8	7.3 ± 0.8	7.9 ± 1.1
<b>Ghrelin (pg/ml)</b>	79 ± 4	83 ± 4	69 ± 3
<b>Cholesterol (mmol/l)</b>	3.1 ± 0.2	3.1 ± 0.1	3.2 ± 0.2
<b>Triglycerides (mmol/l)</b>	0.83 ± 0.07	0.61 ± 0.04*	0.71 ± 0.06*
<b>Free fatty acids (mmol/l)</b>	0.19 ± 0.02	0.76 ± 0.06*	0.83 ± 0.11*
<b>Ketone bodies (mmol/l)</b>	0.11 ± 0.01	0.44 ± 0.06*	1.18 ± 0.26*
<b>T3 (nmol/l)</b>	1.45 ± 0.04	1.44 ± 0.06	1.33 ± 0.06*
<b>FT4 (pmol/l)</b>	15.9 ± 0.6	15.9 ± 0.6	16.6 ± 0.7*
<b>TSH (mU/l)</b>	1.8 ± 0.2	1.4 ± 0.2	1.5 ± 0.2
<b>Testosterone (nmol/l)</b>	19.7 ± 1.1	15.1 ± 1.8*	21.2 ± 2.2
<b>SHBG (nmol/l)</b>	27.2 ± 1.7	28.0 ± 1.7	29.6 ± 1.7*
<b>Cortisol (µmol/l)</b>	0.33 ± 0.03	0.20 ± 0.02*	0.51 ± 0.02*
<b>Alkaline Phosphatase (U/l)</b>	59 ± 5	58 ± 5	64 ± 5*
<b>Creatinine (mmol/l)</b>	71 ± 1	66 ± 2*	76 ± 3*

Data are shown as mean ± SEM, n=12. \*,  $p < 0.05$  vs post-meal ; nd, not determined.

and T3 levels was observed, whereas circulating growth hormone, free fatty acid, ketone bodies, cortisol, alkaline phosphatase and creatinine increased (Table 1).

#### *Effects of fasting on whole-body glucose and lipid oxidation rates*

The substrate oxidation rates were determined by indirect calorimetry at baseline and after 10 and 24 hours of fasting (Table 2). The resting energy expenditure (REE), either expressed as absolute or corrected for lean body mass, remained unaffected throughout the fasting period. As expected, fasting led to significant decrease in respiratory quotient (RQ), indicating a shift in substrate metabolism from glucose toward lipid oxidation (- 48% and +70% after 24h, respectively;  $p < 0.05$ ).

**Table 2. Substrate oxidation rates at baseline and during fasting**

	Post-meal	10h fast	24h fast
<b>Resting energy expenditure (kcal/day)</b>	1627 ± 43	1573 ± 47	1585 ± 70
<b>Resting energy expenditure (kcal/kgFFM/day)</b>	28.8 ± 0.8	27.9 ± 0.8	28.3 ± 1.2
<b>Respiratory quotient</b>	0.99 ± 0.02	0.84 ± 0.02*	0.86 ± 0.03*
<b>Lipid oxidation (μmol/kgFFM/min)</b>	0.49 ± 0.63	4.13 ± 0.50*	3.93 ± 0.70*
<b>Glucose oxidation (μmol/kgFFM/min)</b>	28.2 ± 2.2	13.5 ± 1.9*	14.7 ± 2.0*

Data are shown as mean ± SEM, n=12. \*,  $p < 0.05$  vs post-meal; kgFFM, kilogram fat free mass.

#### *Effect of fasting on insulin/mTORC1 signaling pathways in human skeletal muscle*

The protein expression and phosphorylation state of key molecules involved in the insulin/mTOR signaling pathway were determined in skeletal muscle biopsies at baseline and after 10 and 24h of fasting (Figure 1). Tubulin expression, used as a housekeeping protein, as well as PKB  $\alpha/\beta$ , Akt substrate of 160 kDa (AS160), mTOR, 4Ebinding protein-1 (4E-BP1), S6, ERK1/2, and cAMP response element-binding protein (CREB) were not affected no matter what the conditions (Fig. 1A and data not shown). Although the insulin receptor  $\beta$  (IR $\beta$ ) expression remained unaltered (Figure 1B), the phosphorylation of protein kinase B (PKB, also called Akt) and of its downstream target Akt Substrate of 160 kDa (AS160) were significantly reduced in response to fasting (Figure 1C-D), in line with the time-dependent decrease in plasma insulin levels. In addition, the phosphorylation state of mTOR on its Ser2448 residue was lowered by fasting (Figure 1E), together with phosphorylation of mTOR complex1

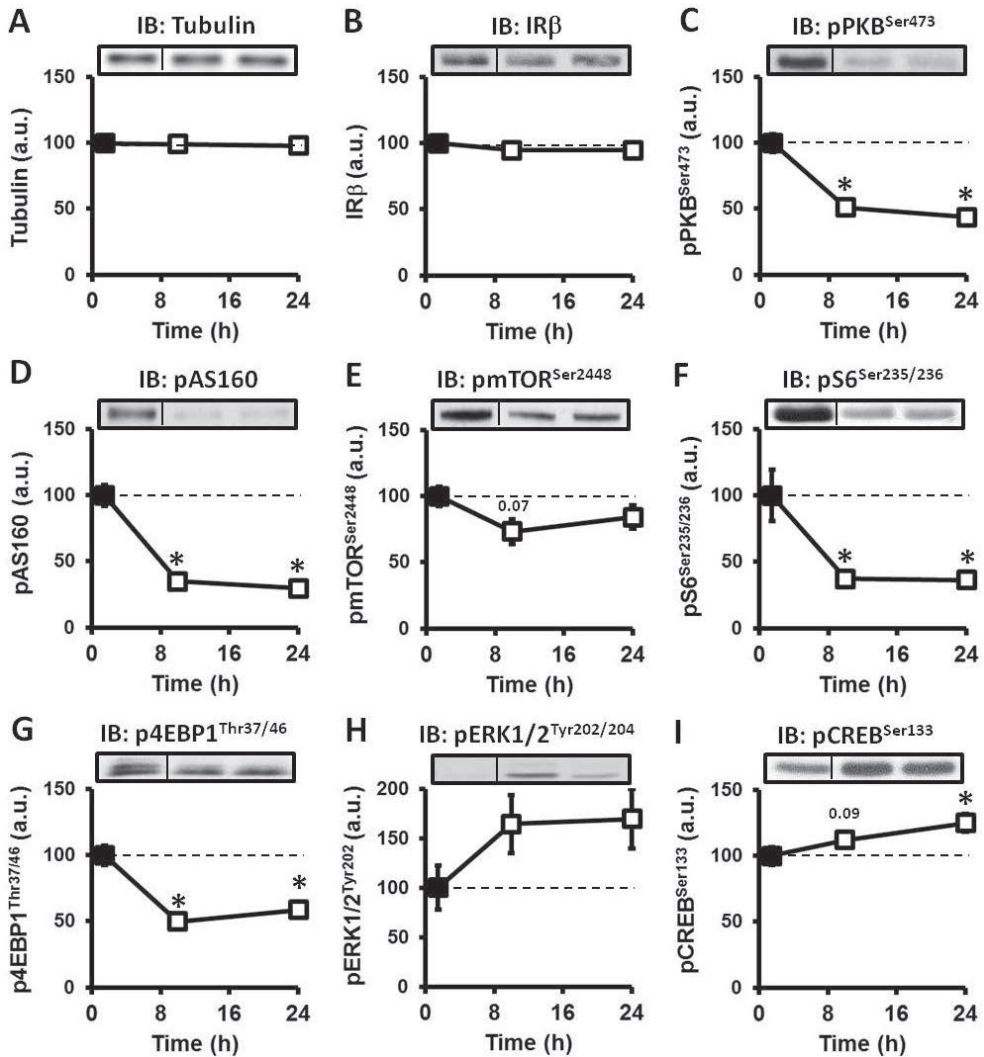


**Figure 1. Effect of fasting on skeletal muscle insulin/mTOR signaling pathways.**

The expression of tubulin (A), insulin receptor  $\beta$  (B) and the phosphorylation states of Ser473-PKB (C), AS160 (D), Ser2448-mTOR (E), Ser235/235-S6 (F), Thr37/46-4EBP1 (G), Tyr202/204-ERK1/2 (H), and Ser133-CREB (I) were assessed by Western Blot in skeletal muscle from healthy subjects before (black square) and after 10h and 24h of fasting (open squares). Representative blots for one subject are shown. Results are normalized to baseline and expressed as mean  $\pm$  SEM;  $n=12$ ; \* $p<0.05$  compared with baseline. IB, immunoblot. a.u., arbitrary units.

(mTORC1) downstream targets ribosomal protein S6 kinase/S6 and eukaryotic initiation factor 4E binding protein (4EBP1) (Figure 1F-G). By contrast, fasting induced a time-dependent increase in both extracellular signal-regulated kinase (ERK) and cAMP response element-binding protein (CREB) phosphorylation on their respective

regulatory residues (Figure 1H-I). Of note, protein expression of PKB $\alpha/\beta$ , AS160, mTOR, 4EBP1, S6, ERK1/2 and CREB were not affected whatever the conditions (*data not shown*).

#### Effect of fasting on AMPK expression and signaling in human skeletal muscle

We next assessed whether fasting affects the protein expression, phosphorylation state and activity of AMPK. As shown in Figure 2A-B, neither AMPK phosphorylation on its activating Thr<sup>172</sup> residue nor AMPK $\alpha$  protein expression differed from baseline after 10 and 24h of fasting. The stoichiometry of AMPK-Thr<sup>172</sup> phosphorylation, assessed by the phosphorylated-to-total protein ratio, was therefore not affected during fasting (Figure 2C). This was confirmed by unchanged AMPK activity measured by kinase assay ( $0.38\pm 0.02$ ,  $0.39\pm 0.02$  and  $0.43\pm 0.03$  mU/mg protein at baseline, 10 and 24h of fasting, respectively). Surprisingly, the phosphorylation state of acetyl-

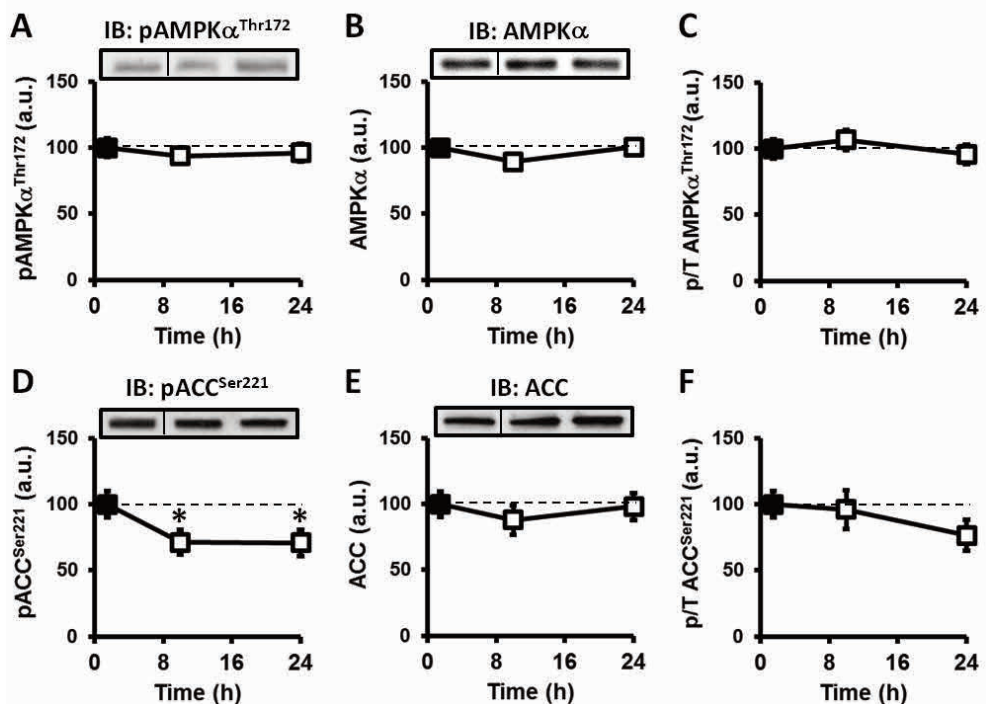


**Figure 2. Effect of fasting on skeletal muscle AMPK signaling.**

The phosphorylation state of Thr<sup>172</sup>-AMPK $\alpha$  (A) and Ser<sup>221</sup>-ACC (D), and the expression of AMPK(pan) $\alpha$  (B) and ACC (E) were assessed by Western Blot in skeletal muscle from healthy subjects before (black square) and after 10h and 24h of fasting (open squares). The phospho-to-total ratio for Thr<sup>172</sup>-AMPK $\alpha$  (C) and Ser<sup>221</sup>-ACC (F) were calculated. Representative blots for one subject are shown. Results are normalized to baseline and expressed as mean  $\pm$  SEM; n=12; \*p<0.05 compared with baseline. IB, immunoblot. a.u., arbitrary units.

CoA carboxylase (ACC) on Ser221, one of the main AMPK downstream targets, was found to be significantly decreased during fasting whereas the expression of ACC was not affected (Figure 2C-D). The stoichiometry of ACC-Ser221 phosphorylation, i.e the phospho-to-total ratio, followed the same pattern although not reaching significance (Figure 2E, -23% at 24h;  $p=0.17$ ). Of note, the mRNA expression of the AMPK upstream kinases liver kinase B (LKB1) and  $\text{Ca}^{2+}$ /calmodulin-dependent protein kinase kinase (CAMKK)  $\alpha/\beta$  and of the different isoforms of AMPK catalytic  $\alpha$  and regulatory  $\beta$  and  $\gamma$  subunits did not change during fasting, except for the AMPK $\gamma$ 3 isoform that was significantly lowered after 24h when compared to baseline (Supplementary Table 1).

#### *Effect of fasting on FoxO1 and SIRT1/HDAC4 histone deacetylases in skeletal muscle*

In addition to the insulin/mTOR and AMPK pathways, other energy/nutrient-sensing pathways, such as FoxO1<sup>9</sup>, SIRT1<sup>11</sup> and HDAC4<sup>12</sup> were also suggested to be involved in the regulation of skeletal muscle substrate metabolism. The fasting-induced changes in skeletal muscle expression and phosphorylation state of these molecules were therefore determined. The phosphorylation of Thr24-FoxO1 was significantly reduced in response to fasting (Figure 3A). Intriguingly, total FoxO1 protein levels were also decreased, leaving the stoichiometry of phosphorylation unaffected and suggesting fasting-induced change in subcellular localization of the protein (Figure 3B-C). The phosphorylation and content of SIRT 1 followed the same pattern as FoxO1, i.e a decrease in response to fasting, although not reaching significance (Figure 3D-F). Furthermore, the phosphorylation of Ser632-HDAC4, but not the protein content, was found to be transiently reduced in skeletal muscle after 10h of fasting (Figure 3G-I).

#### *Effect of fasting on mitochondrial content in skeletal muscle*

Since modulation of nutrient-sensing pathways, including mTOR, AMPK and SIRT1, is linked to regulation of mitochondrial biogenesis, the protein expression of citrate synthase (CS) and of several mitochondrial respiratory-chain complex subunits were determined in skeletal muscle. However, no differences in the expression of these classical markers used for assessing mitochondrial tissue content were observed in response to short-term fasting (Figure 4).

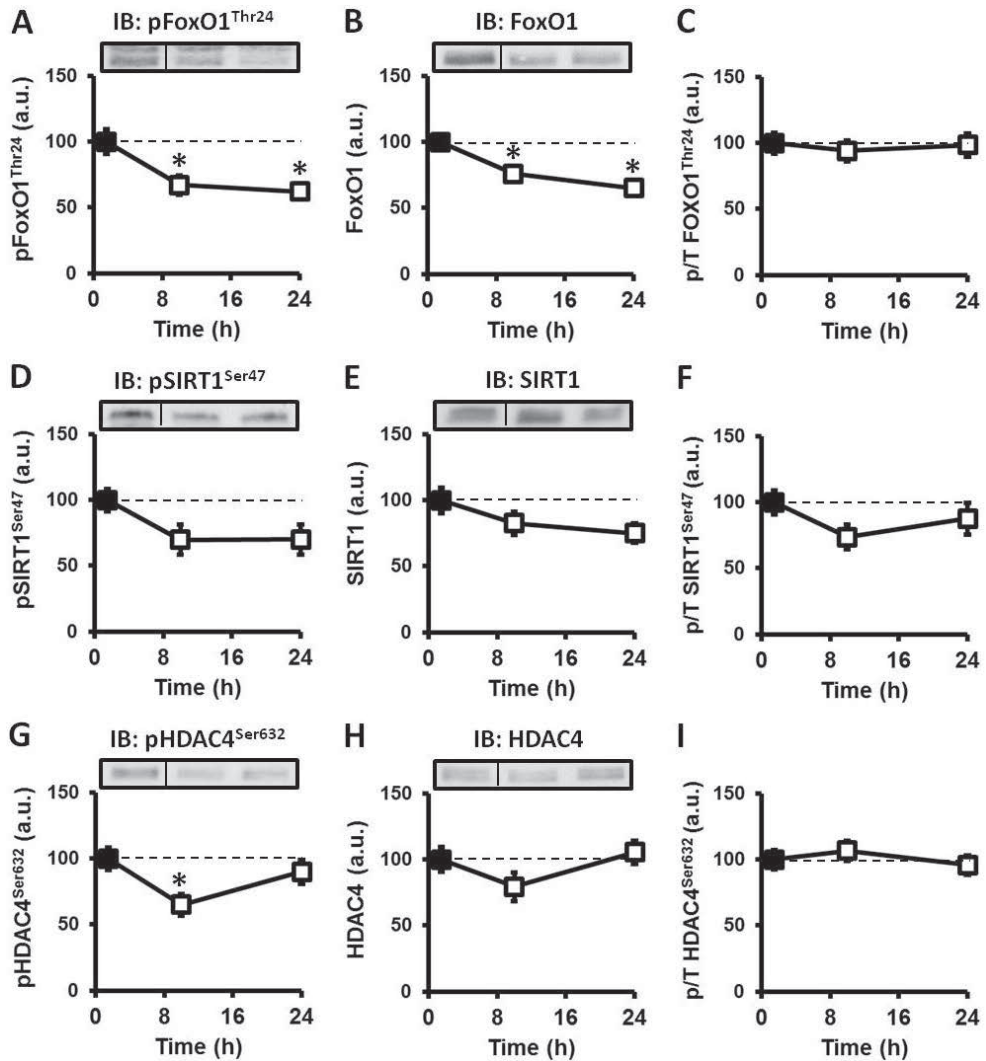


**Figure 3: Effect of fasting on skeletal muscle FoxO1 and histone deacetylases.**

The phosphorylation state of Thr24-FoxO1 (A), Ser47-SIRT1 (D) and Ser632-HDAC4 (G), and expression of FoxO1 (B), SIRT1 (E) and HDAC4 (H) were assessed by Western Blot in skeletal muscle from healthy subjects before (black square) and after 10h and 24h of fasting (open squares). The phospho-to-total ratio for Thr24-FoxO1 (C), Ser47-SIRT1 (F) and Ser632-HDAC4 (I) were calculated. Representative blots for one subject are shown. Results are normalized to baseline and expressed as mean  $\pm$  SEM;  $n=12$ ; \* $p<0.05$  compared with baseline. IB, immunoblot. a.u., arbitrary units.

### *Effect of fasting on skeletal muscle transcriptome*

Gene expression profiling was carried out to gain insight into the mechanisms of the adaptive processes that take place in skeletal muscle during fasting (Figure 5). Among the 34696 genes present on the microarray (47323 transcripts), we found



that 12410 (36 %) were expressed in skeletal muscle in at least one of the samples. Using a detection P value threshold of 0.05 and a Log2 mean fold change lower than 0.75 or higher than 1.25, a total of 44 (24 up-regulated and 20 down-regulated) and 901 (432 up-regulated and 469 down-regulated) differentially expressed genes (DEGs) from baseline were identified after 10 and 24h of fasting, respectively. Analysis of the overlapping DEGs revealed that only 23 genes were significantly affected by fasting at both time points. Microarray data validation of genes selected among the top regulated ones (Table 3) was performed using real-time quantitative PCR (RT-qPCR), confirming the significant changes observed for all the genes tested (Table 4). Finally, to gain insight into the biological implication of the observed transcriptional changes after 10 and 24h of fasting, the significant DEGs were analyzed for over-represented GO terms using the PANTHER® software. Interestingly, the GO anno-

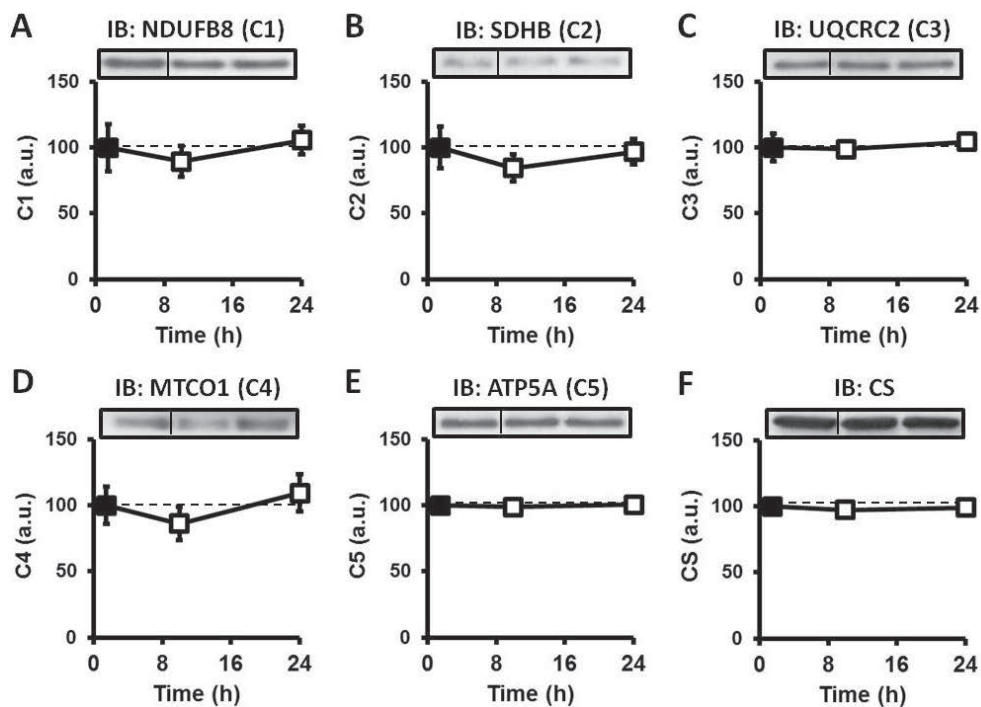


**Figure 4: Effect of fasting on skeletal muscle citrate synthase (CS) and mitochondrial respiratory chain subunit expression**

The expression of various mitochondrial respiratory-chain subunits (A: NDUFB8; B: SDHB; C: UQCRC2; D: MTCO1; E:ATP5A) and CS (F) were assessed by Western Blot in skeletal muscle from healthy subjects before (black square) and after 10h and 24h of fasting (open squares). Representative blots for one subject are shown. Results are normalized to baseline and expressed as mean  $\pm$  SEM; n=12; \*p<0.05 compared with baseline. IB, immunoblot. a.u., arbitrary units.

Table 3. Top 10 up- and down-regulated genes after 10 and 24h of fasting in human skeletal muscle

10h		24h	
Gene symbol	Gene name	Gene symbol	Gene name
<i>Up</i>			
PK4	pyruvate dehydrogenase kinase, isozyme 4	SERPINA3	serpin peptidase inhibitor, clade A, member 3
PFKFB3	6-phosphofructo-2-kinase/fructose-2,6-biphosphatase 3	CEBPD	CCAAT/enhancer binding protein, delta
ANGPTL4	angiopoietin-like 4	HMOX1	heme oxygenase 1
TXNIP	thioredoxin interacting protein	MT2A	metallothionein 2A
NFIL3	nuclear factor, interleukin 3 regulated	GADD45A	growth arrest and DNA-damage-inducible, alpha
CITED2	Chp/β300-interacting transactivator, with Glu/Asp-rich carboxy-terminal domain, 2	PK4	pyruvate dehydrogenase kinase, isozyme 4
UCP3	uncoupling protein 3	PFKFB3	6-phosphofructo-2-kinase/fructose-2,6-biphosphatase 3
PDE4D	phosphodiesterase 4D	NNMT	nicotinamide N-methyltransferase
HDAC4	histone deacetylase 4	SERPINB1	serpin peptidase inhibitor, clade B, member 1
TSC2D1	TSC22 domain family, member 1	RRAD	Ras-related associated with diabetes
<i>Down</i>			
SLC25A25	solute carrier family 25, member 25	SLC25A25	solute carrier family 25, member 25
PER2	period homolog 2	TFRC	transferrin receptor
DBP	D site of albumin promoter binding protein	ACTA2	actin, alpha 2, smooth muscle, aorta
KLF15	Kruppel-like factor 15	SLC16A3	solute carrier family 16, member 3
PER3	period homolog 3	SBK1	SH3-binding domain kinase 1
BHLHB3	basic helix-loop-helix family, member e41	G0S2	G0/G1 switch 2
NR1D2	nuclear receptor subfamily 1, group D, member 2	TAGLN	transgelin
SERTAD3	SERTA domain containing 3	PPARGC1A	peroxisome proliferator-activated receptor gamma, coactivator 1 alpha
TEF	thyrotrophic embryonic factor	FSD2	fibronectin type III and SPRY domain containing 2
PTPN3	protein tyrosine phosphatase, non-receptor type 3	PPP1R3C	protein phosphatase 1, regulatory subunit 3C

Genes are presented by hierarchical order. The whole sets of significantly regulated genes can be found in the Supplementary Table 2.

Table 4. Validation of microarray data by real-time RT-PCR

Gene symbol	Entrez gene	Gene name	10h		24h	
			qPCR	Microarray	qPCR	Microarray
<b>Up</b>						
ANGPTL4	51129	angiopoietin-like 4	3.0 ± 0.5*	1.38*	2.0 ± 0.4*	0.91*
CITED2	187	Cbp/p300-interacting transactivator, with Glu/Asp-rich carboxy-terminal domain 2	1.7 ± 0.4*	1.08*	1.1 ± 0.3*	0.90*
GADD45A	1647	growth arrest and DNA-damage-inducible, alpha	0.9 ± 0.5	1.37	3.5 ± 0.8*	1.85*
PDK4	10777	pyruvate dehydrogenase kinase, isozyme 4	2.4 ± 0.4*	1.93*	2.5 ± 0.5*	1.83*
PFKFB3	10370	6-phosphofructo-2-kinase/fructose-2,6-biphosphatase 3	1.7 ± 0.3*	1.03	2.5 ± 0.5*	1.75*
TXNIP	285527	thioredoxin interacting protein	1.9 ± 0.2*	1.33*	1.7 ± 0.3*	1.21*
UCP3	4783	uncoupling protein 3 (mitochondrial, proton carrier)	0.7 ± 0.2*	0.79*	0.7 ± 0.3*	0.54*
<b>Down</b>						
ARX	170302	aristaless related homeobox	-1.0 ± 0.3*	-0.30*	-2.0 ± 0.3*	-0.36*
ATP2A1	487	ATPase, Ca++ transporting, cardiac muscle, fast twitch 1	-0.2 ± 0.1	-0.26*	-0.3 ± 0.1*	-0.17*
PPARGC1A	10891	peroxisome proliferator-activated receptor gamma, coactivator 1 alpha	-0.6 ± 0.2*	-0.29	-1.7 ± 0.3*	-1.10*
SLC1A7	6512	solute carrier family 1 (glutamate transporter), member 7	-1.7 ± 0.4*	-0.45*	-2.5 ± 0.7*	-0.55*

Data are shown as mean Log2 change vs postmeal condition ± SEM (RT-PCR), n=12. \*, p<0.05 vs post-meal.

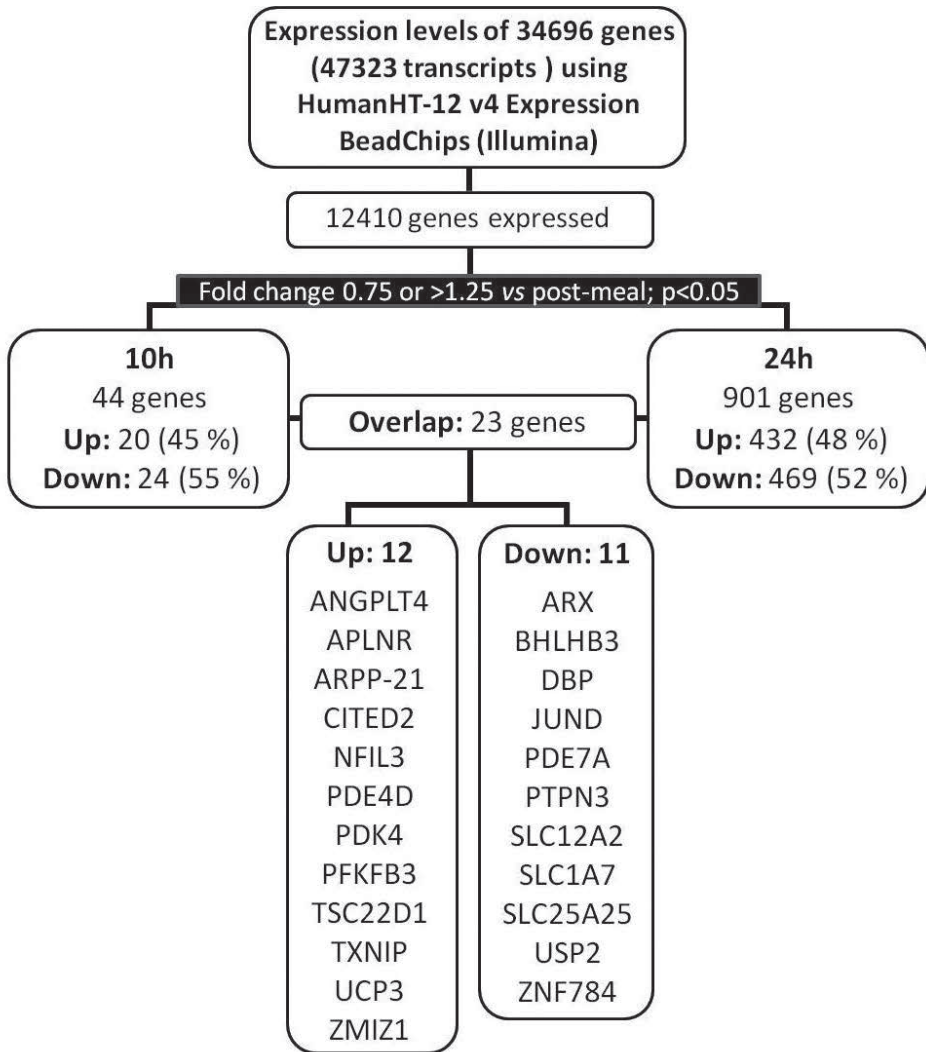


**Figure 5: Flow chart of genes changes during fasting in microarray analysis.**

The complete set of fasting-responsive mRNAs is shown in Supplementary Table 2.

tations found to be significantly over-represented in both gene sets revealed that most of the biological categories identified belonged to the regulation of metabolic processes, although no specific related pathways were identified (Table 5). To note, the GO term “Primary metabolic process” was found to be the only one significantly over-represented in the gene set constituted by the 23 overlapping DEGs ( $p=8.5E-03$ , *data not shown*) when compared to the human skeletal muscle transcriptome.

Table 5. PANTHER gene function categories significantly over-represented in human skeletal muscle gene sets during fasting.

GO Biological Process Category	10h			24h		
	actual	expected	p-value	actual	expected	p-value
acyl-CoA metabolic process	4	0	1.1E-03 (+)	490	411	1.4E-05 (+)
primary metabolic process	42	25	2.3E-03 (+)	417	344	7.4E-05 (+)
fatty acid beta-oxidation	4	0	2.4E-03 (+)	34	13	2.6E-04 (+)
metabolic process	46	29	5.4E-03 (+)	19	5	3.1E-04 (+)
coenzyme metabolic process	5	0	8.0E-03 (+)	27	11	6.6E-03 (+)
generation of precursor metabolites and energy	7	1	1.2E-02 (+)			
protein acetylation	3	0	2.2E-02 (+)			
regulation of biological process	19	8	2.7E-02 (+)			
<b>GO Molecular Function Category</b>						
	10h			24h		
	actual	expected	p-value	actual	expected	p-value
catalytic activity	331	262	6.8E-05 (+)			
G-protein coupled receptor activity	1	14	1.4E-03 (-)			
TGF-beta-activated receptor activity	7	1	2.1E-03 (+)			
transmembrane receptor serine/threonine protein kinase activity	8	1	3.5E-03 (+)			
transferase activity	110	77	2.1E-02 (+)			
cytokine receptor activity	12	3	2.6E-02 (+)			
<b>GO PANTHER Protein Class</b>						
	10h			24h		
	actual	expected	p-value	actual	expected	p-value
G-protein coupled receptor	1	21	1.7E-06 (-)			
TGF-beta receptor	7	1	2.3E-03 (+)			
serine/threonine protein kinase receptor	8	1	1.3E-02 (+)			
actin family cytoskeletal protein	40	21	1.5E-02 (+)			
dehydrogenase	28	12	1.6E-02 (+)			
KRAB box transcription factor	5	19	2.3E-02 (-)			
ribonucleoprotein	16	6	3.6E-02 (+)			
<b>Pathways</b>						
	10h			24h		
	actual	expected	p-value	actual	expected	p-value
Circadian clock system	3	0	1.1E-03 (+)			

The PANTHER classification of biological processes, molecular functions, protein classes and pathways significantly over-represented in differentially expressed gene sets after 10 and 24h of fasting compared to the background set of all genes expressed in human skeletal muscle are shown. The statistical analysis includes a stringent Bonferroni correction for multiple testing. The sign next to the p-value indicates whether the category is enriched (+) or depleted (-) compared to the background gene set for each time point.

Supplementary Table 1. Effects of fasting on skeletal muscle mRNA expression of AMPKs and AMPK subunits

Gene symbol	Entrez gene	Gene name	Mean Log <sub>2</sub> Change	
			10h	24h
<i>CAMKK1</i>	10645	Calcium/calmodulin-dependent protein kinase kinase $\alpha$ (CAMKK $\alpha$ )	0.00	0.06
<i>CAMKK2</i>	84254	Calcium/calmodulin-dependent protein kinase kinase $\beta$ (CAMKK $\beta$ )	-0.08	0.05
<i>CAB39</i>	51719	Calcium binding protein 39 (MO25a)	-0.05	-0.24
<i>CAB39L</i>	81617	Calcium binding protein 39-like (MO25b)	-0.05	-0.05
<i>STRADA</i>	92335	STE20-related kinase adaptor alpha	0.02	-0.06
<i>STK11</i>	6794	Liver Kinase B1 (LKB1)	0.00	-0.03
<i>PRKAA1</i>	5562	AMP-activated protein kinase $\alpha$ 1	0.03	0.10
<i>PRKAA2</i>	5563	AMP-activated protein kinase $\alpha$ 2	0.05	0.10
<i>PRKAB1</i>	5564	AMP-activated protein kinase $\beta$ 1	0.08	0.09
<i>PRKAB2</i>	5565	AMP-activated protein kinase $\beta$ 2	0.06	0.09
<i>PRKAG1</i>	5571	AMP-activated protein kinase $\gamma$ 1	-0.07	-0.19
<i>PRKAG2</i>	51422	AMP-activated protein kinase $\gamma$ 2	0.10	-0.11
<i>PRKAG3</i>	53632	AMP-activated protein kinase $\gamma$ 3	-0.12	-0.38*

Data are shown as mean Log<sub>2</sub> change vs postmeal condition, n=12. \*, p<0.05 vs post-meal.

## Discussion

In the present study, we investigated the time-dependent effects of fasting on whole-body substrate oxidation rates in relation to changes in energy/nutrient-sensing pathways and gene expression in skeletal muscle from healthy men. To our knowledge, this is the first study providing a comprehensive map of the main signal transduction pathways as well as transcriptomic changes during short-term adaptation to fasting in human skeletal muscle.

In healthy individuals who exhibit a high degree of metabolic flexibility, the adaptation to short-term fasting is characterized by a rapid decrease in glucose oxidation associated with a concomitant increase in lipid oxidation by peripheral tissues, mostly in skeletal muscle<sup>1</sup>. In our cohort of lean young men, we observed this expected fasting-induced shift in whole-body substrate metabolism, together with a time-dependent decrease in plasma levels of insulin and leptin, and simultaneous increase in ketone bodies, free fatty acids and growth hormone levels, as previously reported<sup>27,28</sup>. In line with the decrease in circulating insulin levels, we found that the phosphorylation state of (Akt)/PKB was time-dependently reduced by fasting in skeletal muscle, whereas the protein expression of both IR $\beta$  and PKB was not affected. Moreover, the phosphorylation of AS160, one of the main PKB downstream targets, which is involved in the insulin-mediated translocation of the glucose transporter 4 (GLUT4) from intravesicular pool to plasma membrane, was similarly diminished. These findings are in line with our previous report in lean individuals subjected to prolonged (48h) fasting<sup>24</sup> and may suggest that part of the fasting-induced shift from whole-body glucose toward lipid oxidation is secondary to an early reduction of insulin-mediated glucose uptake by skeletal muscle. Of note, Soeters *et al.* did not find significant differences on PKB and AS160 phosphorylation in skeletal muscle from healthy individuals when comparing 14h to 62h of fasting<sup>29</sup>, most likely due to the fact that the inhibition of the pathway was already maximal after 14h.

AMPK is a cellular energy sensor, located at the crossroads of several metabolic pathways, which acts as a master regulator of energy balance. Once activated, AMPK increases insulin-independent glucose uptake, promotes lipid oxidation and enhances mitochondrial biogenesis in skeletal muscle through direct phosphorylation of key regulatory enzymes or transcription factors<sup>30,31</sup>. Since previous studies in rodents have shown that skeletal muscle AMPK is activated in response to fasting<sup>6</sup>, we investigated whether the AMPK pathway was also affected in humans. In the present

study, we did not find any differences in skeletal muscle AMPK expression, phosphorylation and activity after 10 and 24h of fasting when compared to the baseline (post-meal) condition. In line with this finding, Vendelbo *et al.* have recently reported that long-term fasting (72h) did not affect AMPK activity in healthy individuals<sup>32</sup>. As already discussed elsewhere<sup>24</sup>, it is conceivable that fasting-induced AMPK activation constitutes an early regulatory event that transiently occurs in the first hours following food deprivation. Additional experiments including earlier time points are therefore required to clarify this issue.

Another important component in the energy and nutrient-sensing pathways is the mammalian target of rapamycin (mTOR), a kinase that integrates both intracellular and extracellular signals and serves as a central regulator of cell metabolism, growth, proliferation and survival<sup>33</sup>. The mTOR complex 1 (mTORC1), which is one of the two protein complexes containing mTOR, plays an important role in coordinating anabolic and catabolic processes in response to growth factors and nutrients<sup>33</sup>. In response to fasting, we found that phosphorylation of skeletal muscle mTOR and mTORC1 downstream targets S6K/S6 and 4E-BP1 were reduced, an effect which is likely due to reduced PKB signaling. Indeed, active PKB promotes mTORC1 action by phosphorylating and inactivating proline-rich Akt substrate of 40 kDa (PRAS40) and tuberous sclerosis protein 2 (TSC2)<sup>33</sup>. AMPK can also inhibit mTOR signaling by direct phosphorylation of either TSC2<sup>34</sup> or raptor<sup>35</sup>, but the kinase is not likely to be involved in our condition, as its activity was not affected in response to fasting. On top of negatively regulating protein synthesis, one of the most ATP-consuming pathways, mTORC1 controls the transcriptional activity of PPAR $\gamma$  coactivator-1 (PGC1 $\alpha$ ), a nuclear cofactor that regulates mitochondrial biogenesis and oxidative metabolism<sup>36</sup>. Although PPARGC1A (the gene encoding PGC1 $\alpha$ ) was among the most extensively down-regulated transcripts after 24h of fasting, we did not find any obvious differences in other key genes involved in mitochondrial biogenesis, nor in the skeletal muscle protein contents of both CS and the main respiratory-chain complexes subunits. Of note, PGC1  $\alpha$  is not only regulated at the mRNA level but also by post-translational modifications, such as phosphorylation and acetylation<sup>13</sup>, meaning that a decrease in gene expression does not necessarily implicate that its transcriptional activity is switched off.

FoxO1 belongs to a subfamily of the forkhead transcription factors regulating a variety of biological processes, such as metabolism, cell proliferation and differentiation, and stress response<sup>9;37;38</sup>. FoxO1 is phosphorylated by active PKB, thereby causing its



cytoplasmic sequestration through binding to the protein 14-3-3<sup>39</sup>. Thus, in the absence of insulin/growth factors, FoxO1 translocates to the nucleus where it can trigger expression of specific genes. In our condition, we found that the total FoxO1 protein content was rapidly decreased in response to fasting whereas the stoichiometry of phosphorylation of FoxO1 at Thr24, one of the residue directly phosphorylate by active PKB, was not affected. The transcription of FoxO1 was not affected in our condition (data not shown) meaning that the time-dependent decrease observed in FoxO1 should either be due to change in protein stability or in its subcellular localization. FoxO transcription factors are relatively stable proteins which are degraded in a proteasome-dependent manner, notably in response to insulin<sup>40</sup>. As plasma insulin levels are low during fasting, an increase in protein turnover is unlikely, rather suggesting a change in FoxO1 subcellular localization in favor of its nuclear retention. Interestingly, PDK4 which is involved in the regulation of lipid metabolism and up-regulated by fasting<sup>41;42;our study</sup>, has been identified as a FoxO1 target gene in skeletal muscle<sup>43</sup>. Taken together, our finding suggests that the fasting-induced drop in plasma insulin levels might promote FoxO1 nuclear retention, leading to upregulation of FoxO1 target genes, such as PDK4, and ultimately to enhanced skeletal muscle lipid oxidation. Further studies, including extensive analysis of the subcellular localization of skeletal muscle FoxO isoforms in response to fasting, are however required to strengthen this point.

Finally, the deacetylases SIRT1 and HDAC4 were recently shown to be involved in the metabolic shift towards lipid oxidation during fasting in peripheral tissues<sup>11;12</sup>. For instance, SIRT1 can modulate metabolic processes in response to fasting through deacetylation of key transcription factors, such as PGC1  $\alpha$  and FoxO1<sup>44</sup>. The nuclear translocation of SIRT1 and HDAC4, like FoxO1, has been shown to alter the expression of metabolic genes<sup>12;45;46</sup>. As mentioned above, the decrease in SIRT-1 and HDAC4 protein content in response to fasting likely results from their nuclear translocation upon dephosphorylation. Further studies are however required to strengthen this finding.

In the present study, we reported that more than 900 genes were altered in human skeletal muscle after 24h of fasting representing ~7% of the genes expressed in this tissue. However, only 23 genes, mostly involved in the regulation of metabolic processes, were found to be significantly affected by fasting at both early (10h) and late (24h) time points. Some of them have previously been reported to be up-regulated (ANGPLT4, CITED2, PDK4, PFKFB3, TXNIP and UCP3) or down-regulated

(SLC25A25) in response to fasting in human skeletal muscle and are likely contributing to the shift from glucose to lipid oxidation at the whole-body level <sup>41,42,47,48</sup>. In addition, we identified new candidate genes that are rapidly and consistently affected by fasting, suggesting that they might also play a role in the initial adaptation of skeletal muscle to energy deprivation. Unfortunately, few data are available on the functions of most of these genes, especially with respect to skeletal muscle. Among them, the APLNR gene encoding the apelin receptor was found to be significantly up-regulated in response to fasting <sup>49</sup>. Interestingly, the expression of APLNR has been shown to be reduced in skeletal muscle from both high-fat fed and db/db mice <sup>50</sup>, whereas apelin treatment increases FA oxidation, mitochondrial oxidative capacity, and biogenesis in muscle of insulin-resistant mice <sup>51</sup>. In addition, some genes involved in the cAMP (ARPP-21, PDE4D, PDE7A) or TGF $\beta$  (TSC22D1, ZMIZ1) signaling pathways, which play crucial roles in the regulation of multiple cellular functions and physiological processes in skeletal muscle, were also found to be regulated by fasting. Clearly, additional studies are required to investigate whether these proteins are actually involved in the skeletal muscle metabolic adaptation to fasting, and whether specific or common upstream pathways mediated their transcriptional regulation. Among the study limitations, we cannot exclude that some of the effects of fasting on signal transduction and/or protein/gene expression we observed are specific to *musculus vastus lateralis*, which contains a mix of slow and fast fibers, and would have been different in muscles with other fiber type composition. In addition, the only pathway that was found to be significantly over-represented in the two gene sets was the circadian clock after 10h of fasting. Although very little is known in skeletal muscle, the core molecular clock plays an important role in the transcriptional regulation of metabolic processes <sup>52</sup>. It is therefore conceivable that some of the changes observed in gene expression can partly be secondary to circadian rhythms. Collectively, our study provides a comprehensive map of the main energy/nutrient-sensing pathways and transcriptomic changes during short-term adaptation to fasting in human skeletal muscle. Future studies are necessary to determine whether the observed changes are relevant in disease development as well as (healthy) aging and longevity.

---

## References

1. Soeters MR, Soeters PB, Schooneman MG, Houten SM, Romijn JA. Adaptive reciprocity of lipid and glucose metabolism in human short-term starvation. *Am J Physiol Endocrinol Metab* 2012; 303(12): E1397-E1407.
2. de LP, Moreno M, Silvestri E, Lombardi A, Goglia F, Lanni A. Fuel economy in food-deprived skeletal muscle: signaling pathways and regulatory mechanisms. *FASEB J* 2007; 21(13): 3431-3441.
3. Steinberg GR, Kemp BE. AMPK in Health and Disease. *Physiol Rev* 2009; 89(3): 1025-1078.
4. Carling D, Thornton C, Woods A, Sanders MJ. AMP-activated protein kinase: new regulation, new roles? *Biochem J* 2012; 445(1): 11-27.
5. Hardie DG, Ross FA, Hawley SA. AMPK: a nutrient and energy sensor that maintains energy homeostasis. *Nat Rev Mol Cell Biol* 2012; 13(4): 251-262.
6. de LP, Farina P, Moreno M, Ragni M, Lombardi A, Silvestri E, Burrone L, Lanni A, Goglia F. Sequential changes in the signal transduction responses of skeletal muscle following food deprivation. *FASEB J* 2006; 20(14): 2579-2581.
7. Canto C, Jiang LQ, Deshmukh AS, Matakı C, Coste A, Lagouge M, Zierath JR, Auwerx J. Interdependence of AMPK and SIRT1 for metabolic adaptation to fasting and exercise in skeletal muscle. *Cell Metab* 2010; 11(3): 213-219.
8. Um SH, Frigerio F, Watanabe M, Picard F, Joaquin M, Sticker M, Fumagalli S, Allegrini PR, Kozma SC, Auwerx J, Thomas G. Absence of S6K1 protects against age- and diet-induced obesity while enhancing insulin sensitivity. *Nature* 2004; 431(7005): 200-205.
9. Gross DN, van den Heuvel AP, Birnbaum MJ. The role of FoxO in the regulation of metabolism. *Oncogene* 2008; 27(16): 2320-2336.
10. Lovreglio P, Carrieri M, Barbieri A, Sabatini L, Fustinoni S, Andreoli R, D'Errico MN, Basso A, Bartolucci GB, Soleo L. [Monitoring of the occupational and environmental exposure to low doses of benzene]. *G Ital Med Lav Ergon* 2013; 35(4): 251-255.
11. Gerhart-Hines Z, Rodgers JT, Bare O, Lerin C, Kim SH, Mostoslavsky R, Alt FW, Wu Z, Puigserver P. Metabolic control of muscle mitochondrial function and fatty acid oxidation through SIRT1/PGC-1alpha. *EMBO J* 2007; 26(7): 1913-1923.
12. Mihaylova MM, Vasquez DS, Ravnskjaer K, Denechaud PD, Yu RT, Alvarez JG, Downes M, Evans RM, Montminy M, Shaw RJ. Class IIa histone deacetylases

- are hormone-activated regulators of FOXO and mammalian glucose homeostasis. *Cell* 2011; 145(4): 607-621.
13. Canto C, Auwerx J. PGC-1alpha, SIRT1 and AMPK, an energy sensing network that controls energy expenditure. *Curr Opin Lipidol* 2009; 20(2): 98-105.
  14. Mihaylova MM, Shaw RJ. The AMPK signalling pathway coordinates cell growth, autophagy and metabolism. *Nat Cell Biol* 2011; 13(9): 1016-1023.
  15. Inoki K, Kim J, Guan KL. AMPK and mTOR in cellular energy homeostasis and drug targets. *Annu Rev Pharmacol Toxicol* 2012; 52: 381-400.
  16. Fontana L, Partridge L, Longo VD. Extending healthy life span—from yeast to humans. *Science* 2010; 328(5976): 321-326.
  17. Greer EL, Brunet A. Signaling networks in aging. *J Cell Sci* 2008; 121(Pt 4): 407-412.
  18. Chalkiadaki A, Guarente L. Sirtuins mediate mammalian metabolic responses to nutrient availability. *Nat Rev Endocrinol* 2012; 8(5): 287-296.
  19. Lapierre LR, Hansen M. Lessons from *C. elegans*: signaling pathways for longevity. *Trends Endocrinol Metab* 2012; 23(12): 637-644.
  20. Yuan HX, Xiong Y, Guan KL. Nutrient sensing, metabolism, and cell growth control. *Mol Cell* 2013; 49(3): 379-387.
  21. Snel M, Jonker JT, Hammer S, Kerpershoek G, Lamb HJ, Meinders AE, Pijl H, de RA, Romijn JA, Smit JW, Jazet IM. Long-term beneficial effect of a 16-week very low calorie diet on pericardial fat in obese type 2 diabetes mellitus patients. *Obesity (Silver Spring)* 2012; 20(8): 1572-1576.
  22. Kok P, Roelfsema F, Frolich M, van PJ, Stokkel MP, Meinders AE, Pijl H. Activation of dopamine D2 receptors simultaneously ameliorates various metabolic features of obese women. *Am J Physiol Endocrinol Metab* 2006; 291(5): E1038-E1043.
  23. Stephenne X, Foretz M, Taleux N, van der Zon GC, Sokal E, Hue L, Viollet B, Guigas B. Metformin activates AMP-activated protein kinase in primary human hepatocytes by decreasing cellular energy status. *Diabetologia* 2011; 54(12): 3101-3110.
  24. Wijngaarden MA, van der Zon GC, van Dijk KW, Pijl H, Guigas B. Effects of prolonged fasting on AMPK signaling, gene expression, and mitochondrial respiratory chain content in skeletal muscle from lean and obese individuals. *Am J Physiol Endocrinol Metab* 2013; 304(9): E1012-E1021.
  25. Du P, Kibbe WA, Lin SM. lumi: a pipeline for processing Illumina microarray. *Bioinformatics* 2008; 24(13): 1547-1548.

26. Mi H, Muruganujan A, Casagrande JT, Thomas PD. Large-scale gene function analysis with the PANTHER classification system. *Nat Protoc* 2013; 8(8): 1551-1566.
27. Webber J, Macdonald IA. The cardiovascular, metabolic and hormonal changes accompanying acute starvation in men and women. *Br J Nutr* 1994; 71(3): 437-447.
28. Chan JL, Heist K, DePaoli AM, Veldhuis JD, Mantzoros CS. The role of falling leptin levels in the neuroendocrine and metabolic adaptation to short-term starvation in healthy men. *J Clin Invest* 2003; 111(9): 1409-1421.
29. Soeters MR, Sauerwein HP, Dubbelhuis PF, Groener JE, Ackermans MT, Fliers E, Aerts JM, Serlie MJ. Muscle adaptation to short-term fasting in healthy lean humans. *J Clin Endocrinol Metab* 2008; 93(7): 2900-2903.
30. Viollet B, Athesa Y, Mounier R, Guigas B, Zarrinpashneh E, Horman S, Lantier L, Hebrard S, Devin-Leclerc J, Beauloye C, Foretz M, Andreelli F, Ventura-Clapier R, Bertrand L. AMPK: Lessons from transgenic and knockout animals. *Front Biosci (Landmark Ed)* 2009; 14: 19-44.
31. Hardie DG. Energy sensing by the AMP-activated protein kinase and its effects on muscle metabolism. *Proc Nutr Soc* 2011; 70(1): 92-99.
32. Vendelbo MH, Clasen BF, Trebak JT, Moller L, Krusenstjerna-Hafstrom T, Madsen M, Nielsen TS, Stodkilde-Jorgensen H, Pedersen SB, Jorgensen JO, Goodyear LJ, Wojtaszewski JF, Moller N, Jessen N. Insulin Resistance after a 72 hour Fast is Associated with Impaired AS160 Phosphorylation and Accumulation of Lipid and Glycogen in Human Skeletal Muscle. *Am J Physiol Endocrinol Metab* 2011.
33. Laplante M, Sabatini DM. Regulation of mTORC1 and its impact on gene expression at a glance. *J Cell Sci* 2013; 126(Pt 8): 1713-1719.
34. Inoki K, Li Y, Zhu T, Wu J, Guan KL. TSC2 is phosphorylated and inhibited by Akt and suppresses mTOR signalling. *Nat Cell Biol* 2002; 4(9): 648-657.
35. Gwinn DM, Shackelford DB, Egan DF, Mihaylova MM, Mery A, Vasquez DS, Turk BE, Shaw RJ. AMPK phosphorylation of raptor mediates a metabolic checkpoint. *Mol Cell* 2008; 30(2): 214-226.
36. Cunningham JT, Rodgers JT, Arlow DH, Vazquez F, Mootha VK, Puigserver P. mTOR controls mitochondrial oxidative function through a YY1-PGC-1alpha transcriptional complex. *Nature* 2007; 450(7170): 736-740.
37. Greer EL, Brunet A. FOXO transcription factors in ageing and cancer. *Acta Phys-*

- 
- iol (Oxf)* 2008; 192(1): 19-28.
38. Hay N. Interplay between FOXO, TOR, and Akt. *Biochim Biophys Acta* 2011; 1813(11): 1965-1970.
  39. Rena G, Guo S, Cichy SC, Unterman TG, Cohen P. Phosphorylation of the transcription factor forkhead family member FKHR by protein kinase B. *J Biol Chem* 1999; 274(24): 17179-17183.
  40. Calnan DR, Brunet A. The FoxO code. *Oncogene* 2008; 27(16): 2276-2288.
  41. Pilegaard H, Saltin B, Neufer PD. Effect of short-term fasting and refeeding on transcriptional regulation of metabolic genes in human skeletal muscle. *Diabetes* 2003; 52(3): 657-662.
  42. Tsintzas K, Jewell K, Kamran M, Laithwaite D, Boonsong T, Littlewood J, Macdonald I, Bennett A. Differential regulation of metabolic genes in skeletal muscle during starvation and refeeding in humans. *J Physiol* 2006; 575(Pt 1): 291-303.
  43. Furuyama T, Kitayama K, Yamashita H, Mori N. Forkhead transcription factor FOXO1 (FKHR)-dependent induction of PDK4 gene expression in skeletal muscle during energy deprivation. *Biochem J* 2003; 375(Pt 2): 365-371.
  44. Canto C, Auwerx J. Targeting sirtuin 1 to improve metabolism: all you need is NAD(+)? *Pharmacol Rev* 2012; 64(1): 166-187.
  45. Finkel T, Deng CX, Mostoslavsky R. Recent progress in the biology and physiology of sirtuins. *Nature* 2009; 460(7255): 587-591.
  46. Wang B, Moya N, Niessen S, Hoover H, Mihaylova MM, Shaw RJ, Yates JR, III, Fischer WH, Thomas JB, Montminy M. A hormone-dependent module regulating energy balance. *Cell* 2011; 145(4): 596-606.
  47. Tunstall RJ, Mehan KA, Hargreaves M, Spriet LL, Cameron-Smith D. Fasting activates the gene expression of UCP3 independent of genes necessary for lipid transport and oxidation in skeletal muscle. *Biochem Biophys Res Commun* 2002; 294(2): 301-308.
  48. Kunkel SD, Suneja M, Ebert SM, Bongers KS, Fox DK, Malmberg SE, Alipour F, Shields RK, Adams CM. mRNA expression signatures of human skeletal muscle atrophy identify a natural compound that increases muscle mass. *Cell Metab* 2011; 13(6): 627-638.
  49. Boucher J, Masri B, Daviaud D, Gesta S, Guigne C, Mazzucotelli A, Castan-Lauréll I, Tack I, Knibiehler B, Carpené C, Audigier Y, Saulnier-Blache JS, Valet P. Apelin, a newly identified adipokine up-regulated by insulin and obesity. *Endocrinology* 2005; 146(4): 1764-1771.
-

50. Dray C, Debard C, Jager J, Disse E, Daviaud D, Martin P, Attane C, Wanecq E, Guigne C, Bost F, Tanti JF, Laville M, Vidal H, Valet P, Castan-Laurell I. Apelin and APJ regulation in adipose tissue and skeletal muscle of type 2 diabetic mice and humans. *Am J Physiol Endocrinol Metab* 2010; 298(6): E1161-E1169.
51. Attane C, Foussal C, Le GS, Benani A, Daviaud D, Wanecq E, Guzman-Ruiz R, Dray C, Bezaire V, Rancoule C, Kuba K, Ruiz-Gayo M, Levade T, Penninger J, Burcelin R et al. Apelin treatment increases complete Fatty Acid oxidation, mitochondrial oxidative capacity, and biogenesis in muscle of insulin-resistant mice. *Diabetes* 2012; 61(2): 310-320.
52. Doherty CJ, Kay SA. Circadian control of global gene expression patterns. *Annu Rev Genet* 2010; 44: 419-444.

## Acknowledgements

The authors are grateful to Jan van Klinken for his help on statistical analysis.

**Supplementary Table 2**  
mRNAs regulated by fasting in human skeletal muscle, as assessed by exon expression arrays  
The table includes all mRNAs whose levels were increased (gray) or decreased (black) by fasting ( $P \leq 0.02$  by paired t-test).

<b>EntrezID</b>	<b>Symbol</b>	<b>Gene Name</b>	<b>Mean Log2 Change</b>	<b>AdjPvalue</b>
<b>10h</b>				
5166	PDK4	pyruvate dehydrogenase kinase, isozyme 4	1,93	0,00
5209	PFKFB3	6-phosphofructo-2-kinase/fructose-2,6-biphosphatase 3	1,59	0,02
51129	ANGPTL4	angiopoietin-like 4	1,38	0,01
10628	TXNIP	thioredoxin interacting protein	1,33	0,00
4783	NFIL3	nuclear factor, interleukin 3 regulated	1,16	0,05
10370	CITED2	Cbp/p300-interacting transactivator, with Glu/Asp-rich carboxy-terminal domain, 2	1,08	0,01
7352	UCP3	uncoupling protein 3 (mitochondrial, proton carrier)	0,79	0,02
5144	PDE4D	phosphodiesterase 4D, cAMP-specific (phosphodiesterase E3 duncce homolog, Drosophila)	0,55	0,01
9759	HDAC4	histone deacetylase 4	0,52	0,00
8848	TSC22D1	TSC22 domain family, member 1	0,48	0,01
406	ARN1L	aryl hydrocarbon receptor nuclear translocator-like	0,46	0,02
1195	CLK1	CDC-like kinase 1	0,45	0,02
187	APLN	apelin receptor	0,42	0,00
220963	SLC16A9	solute carrier family 16, member 9 (monocarboxylic acid transporter 9)	0,40	0,00
114818	KLHL29	kelch-like 29 (Drosophila)	0,40	0,01
57178	ZMIZ1	zinc finger, MIZ-type containing 1	0,40	0,00
10777	ARPP-21	cyclic AMP-regulated phosphoprotein, 21 kD	0,32	0,03
79843	FAM124B	family with sequence similarity 124B	0,29	0,00
56243	KIAA1217	KIAA1217	0,29	0,03
4649	MYO9A	myosin IXA	0,26	0,05
<b>5898</b>	<b>RALA</b>	<b>v-ral simian leukemia viral oncogene homolog A (ras related)</b>	<b>-0,26</b>	<b>0,00</b>



487	ATP2A1	ATPase, Ca++ transporting, cardiac muscle, fast twitch 1	-0,26	0,01
170302	ARX	aristalless related homeobox	-0,30	0,01
23462	HEY1	hairy/enhancer-of-split related with YRPW motif 1	-0,34	0,02
89797	NAV2	neuron navigator 2	-0,36	0,00
9099	USP2	ubiquitin specific peptidase 2	-0,37	0,01
79971	GPR177	G protein-coupled receptor 177	-0,37	0,00
23355	VPS8	vacuolar protein sorting 8 homolog ( <i>S. cerevisiae</i> )	-0,38	0,01
147808	ZNF784	zinc finger protein 784	-0,39	0,05
5150	PDE7A	phosphodiesterase 7A	-0,41	0,02
7088	TLE1	similar to transducin-like enhancer of split 1 (E(spl) homolog, <i>Drosophila</i> ); transducin-like enhancer of split 1 (E(spl) homolog, <i>Drosophila</i> )	-0,41	0,05
6558	SLC12A2	solute carrier family 12 (sodium/potassium/chloride transporters), member 2	-0,45	0,01
3727	JUND	jun D proto-oncogene	-0,45	0,03
6512	SLC1A7	solute carrier family 1 (glutamate transporter), member 7	-0,45	0,00
5774	PTPN3	protein tyrosine phosphatase, non-receptor type 3	-0,46	0,04
7008	TEF	thyrotrophic embryonic factor	-0,47	0,03
29946	SERTAD3	SERTA domain containing 3	-0,50	0,00
9975	NR1D2	nuclear receptor subfamily 1, group D, member 2	-0,53	0,00
79365	BHLHB3	basic helix-loop-helix family, member e41	-0,57	0,01
8863	PER3	period homolog 3 ( <i>Drosophila</i> )	-0,58	0,00
28999	KLF15	Kruppel-like factor 15	-0,66	0,00
1628	DBP	D site of albumin promoter (albumin D-box) binding protein	-0,77	0,00
8864	PER2	period homolog 2 ( <i>Drosophila</i> )	-0,78	0,03
114789	SLC25A25	solute carrier family 25 (mitochondrial carrier; phosphate carrier), member 25	-1,59	0,00
24h				
<b>EntrezID</b>	<b>Symbol</b>	<b>Gene Name</b>	<b>Mean Log2 Change</b>	<b>AdjPvalue</b>
12	SERPINA3	serpin peptidase inhibitor, clade A (alpha-1 antiproteinase, antitrypsin), member 3	2,27	0,02

1052	CEBPD	CCAAT/enhancer binding protein (C/EBP), delta	2,15	0,00
3162	HMOX1	heme oxygenase (decycling) 1	2,05	0,00
4502	MT2A	metallothionein 2A	1,93	0,00
1647	GADD45A	growth arrest and DNA-damage-inducible, alpha	1,85	0,01
5166	PDK4	pyruvate dehydrogenase kinase, isozyme 4	1,83	0,00
5209	PFKFB3	6-phosphofructo-2-kinase/fructose-2,6-biphosphatase 3	1,75	0,00
4837	NNMT	nicotinamide N-methyltransferase	1,73	0,01
1992	SERPINB1	serpin peptidase inhibitor, clade B (ovalbumin), member 1	1,71	0,02
6236	RRAD	Ras-related associated with diabetes	1,69	0,04
4609	MYC	v-myc myelocytomatosis viral oncogene homolog (avian)	1,67	0,03
5142	PDE4B	phosphodiesterase 4B, cAMP-specific (phosphodiesterase E4 dunce homolog, Drosophila)	1,55	0,02
70	ACTC1	actin, alpha, cardiac muscle 1	1,44	0,01
23516	SLC39A14	solute carrier family 39 (zinc transporter), member 14	1,28	0,02
5621	PRNP	prion protein	1,23	0,00
10628	TXNIP	thioredoxin interacting protein	1,21	0,00
4489	MT1A	metallothionein 1A	1,20	0,00
23109	DDN	dendrin	1,16	0,00
10135	NAMPT	nicotinamide phosphoribosyltransferase	1,11	0,02
29982	NRBF2	nuclear receptor binding factor 2	1,06	0,01
29970	SCHIP1	schwannomin interacting protein 1	1,03	0,00
8048	CSRP3	cysteine and glycine-rich protein 3 (cardiac LIM protein)	1,02	0,00
4783	NFIL3	nuclear factor, interleukin 3 regulated	0,99	0,02
1545	CYP11B1	cytochrome P450, family 1, subfamily B, polypeptide 1	0,99	0,02
9188	DDX21	DEAD (Asp-Glu-Ala-Asp) box polypeptide 21	0,98	0,01
58480	RHOU	ras homolog gene family, member U	0,98	0,03
123	PLIN2	adipose differentiation-related protein	0,95	0,01
9976	CLEC2B	C-type lectin domain family 2, member B	0,95	0,00
644314	MTE	metallothionein II (pseudogene)	0,94	0,00
3929	LBP	lipopolysaccharide binding protein	0,92	0,01
4493	MT1E	metallothionein 1E; metallothionein 1 pseudogene	0,91	0,00

			3; metallothionein 1J (pseudogene)		
51129	ANGPTL4		angiotensin-like 4	0,91	0,03
2745	GLRX		glutaredoxin (thioltransferase)	0,91	0,00
10370	CITED2		Cbp/p300-interacting transactivator, with Glu/Asp-rich carboxy-terminal domain, 2	0,90	0,01
84676	TRIM63		tripartite motif-containing 63	0,89	0,04
4618	MYF6		myogenic factor 6 (herculin)	0,87	0,01
4501	MT1X		metallothionein 1X	0,87	0,00
144453	BEST3		bestrophin 3	0,86	0,00
124935	SLC43A2		solute carrier family 43, member 2	0,86	0,00
7132	TNFRSF1A		tumor necrosis factor receptor superfamily, member 1A	0,85	0,02
2634	GBP2		guanylate binding protein 2, interferon-inducible	0,85	0,00
11142	PKIG		protein kinase (cAMP-dependent, catalytic) inhibitor gamma	0,85	0,00
7122	CLDN5		claudin 5	0,85	0,00
10410	IFITM3		interferon induced transmembrane protein 3 (1-8U)	0,83	0,02
58526	MID1IP1		MID1 interacting protein 1 (gastrulation specific G12 homolog (zebrafish))	0,82	0,01
2114	ETS2		v-ets erythroblastosis virus E26 oncogene homolog 2 (avian)	0,82	0,03
56975	FAM20C		family with sequence similarity 20, member C	0,81	0,01
6648	SOD2		superoxide dismutase 2, mitochondrial	0,79	0,03
55281	TMEM140		transmembrane protein 140	0,79	0,00
23082	PPRC1		peroxisome proliferator-activated receptor gamma, coactivator-related 1	0,79	0,04
7371	UCK2		uridine-cytidine kinase 2	0,77	0,01
602	BCL3		B-cell CLL/lymphoma 3	0,77	0,05
9903	KLHL21		kelch-like 21 (Drosophila)	0,77	0,00
23452	ANGPTL2		angiotensin-like 2	0,77	0,02
6547	SLC8A3		solute carrier family 8 (sodium/calcium exchanger), member 3	0,77	0,00
54438	GFOD1		glucose-fructose oxidoreductase domain containing 1	0,77	0,01
861	RUNX1		runt-related transcription factor 1	0,77	0,03
3987	LIMS1		LIM and senescent cell antigen-like domains 1	0,75	0,00
694	BTG1		B-cell translocation gene 1, anti-proliferative	0,74	0,00
7494	XBP1		X-box binding protein 1	0,71	0,01

83786	FRMD8	FERM domain containing 8	0,71	0,03
10581	IFITM2	interferon induced transmembrane protein 2 (1-8D)	0,71	0,04
5918	RARRES1	retinoic acid receptor responder (tazarotene induced) 1	0,70	0,04
26267	FBXO10	F-box protein 3	0,70	0,00
7045	TGFB1	transforming growth factor, beta-induced, 68kDa	0,70	0,01
57132	CHMP1B	chromatin modifying protein 1B	0,70	0,00
11177	BAZ1A	bromodomain adjacent to zinc finger domain, 1A	0,69	0,00
23710	GABARAPL1	GABA(A) receptors associated protein like 3 (pseudogene); GABA(A) receptor-associated protein like 1	0,69	0,02
64786	TBC1D15	TBC1 domain family, member 15	0,68	0,00
8848	TSC22D1	TSC22 domain family, member 1	0,68	0,00
3487	IGFBP4	insulin-like growth factor binding protein 4	0,67	0,00
26354	GNL3	cyclin M4	0,67	0,01
705	BYSL	bystin-like	0,66	0,00
2512	FTL	similar to ferritin, light polypeptide; ferritin, light polypeptide	0,66	0,01
3656	IRAK2	interleukin-1 receptor-associated kinase 2	0,66	0,00
9334	B4GALT5	UDP-Gal:betaGlcNAc beta 1,4- galactosyltransferase, polypeptide 5	0,65	0,03
4780	NFE2L2	nuclear factor (erythroid-derived 2)-like 2	0,65	0,00
4217	MAP3K5	mitogen-activated protein kinase kinase kinase 5	0,64	0,03
7763	ZFAND5	similar to zinc finger, AN1-type domain 5; zinc finger, AN1-type domain 5	0,64	0,00
377007	KLHL30	kelch-like 30 (Drosophila)	0,64	0,00
303	ANXA2P1	annexin A2 pseudogene 3; annexin A2; annexin A2 pseudogene 1	0,63	0,02
7103	TSPAN8	tetraspanin 8	0,63	0,00
7465	WEE1	WEE1 homolog (S. pombe)	0,63	0,00
51491	NOPI6	NOPI6 nucleolar protein homolog (yeast)	0,62	0,02
79026	AHNAK	AHNAK nucleoprotein	0,62	0,00
4234	METTL1	methyltransferase like 1	0,61	0,03
64778	FNDC3B	fibronectin type III domain containing 3B	0,61	0,01
476	ATP1A1	ATPase, Na+/K+ transporting, alpha 1 polypeptide	0,61	0,04
2878	GPX3	glutathione peroxidase 3 (plasma)	0,61	0,02

54880	BCOR	BCL6 co-repressor	0,61	0,00
24145	PANX1	pannexin 1	0,60	0,03
27106	ARRDC2	arrestin domain containing 2	0,60	0,00
84365	MKI67IP	MKI67 (FHA domain) interacting nucleolar phosphoprotein	0,59	0,02
2730	GCLM	glutamate-cysteine ligase, modifier subunit	0,59	0,00
396	ARHGDI1A	Rho GDP dissociation inhibitor (GDI) alpha	0,59	0,01
55636	CHD7	chromodomain helicase DNA binding protein 7	0,58	0,02
6890	TAP1	transporter 1, ATP-binding cassette, sub-family B (MDR/TAP)	0,58	0,03
84888	SPPL2A	signal peptide peptidase-like 2A	0,58	0,01
55608	ANKRD10	ankyrin repeat domain 10	0,58	0,01
1497	CTNS	cystinosis, nephropathic	0,58	0,02
10057	ABCC5	ATP-binding cassette, sub-family C (CFTR/MRP), member 5	0,57	0,00
8519	IFITM1	interferon induced transmembrane protein 1 (9-27)	0,57	0,02
55174	INTS10	integrator complex subunit 10	0,57	0,02
1950	EGF	epidermal growth factor (beta-urogastrone)	0,57	0,00
604	BCL6	B-cell CLL/lymphoma 6	0,56	0,01
6776	STAT5A	signal transducer and activator of transcription 5A	0,56	0,01
57563	KLHL8	kelch-like 8 (Drosophila)	0,55	0,00
196527	ANO6	anoctamin 6	0,55	0,00
84448	ABLIM2	actin binding LIM protein family, member 2	0,55	0,02
55240	STEAP3	STEAP family member 3	0,55	0,02
677838	SNORA61	small nucleolar RNA, H/ACA box 61	0,55	0,05
79080	CCDC86	coiled-coil domain containing 86	0,55	0,00
8511	MMP23A	matrix metalloproteinase 23A (pseudogene); matrix metalloproteinase 23B	0,55	0,01
5770	PTPN1	protein tyrosine phosphatase, non-receptor type 1	0,54	0,03
1729	DIAPH1	diaphanous homolog 1 (Drosophila)	0,54	0,00
23612	PHLDA3	pleckstrin homology-like domain, family A, member 3	0,54	0,00
7352	UCP3	uncoupling protein 3 (mitochondrial, proton carrier)	0,54	0,00
7351	UCP2	uncoupling protein 2 (mitochondrial, proton carrier)	0,53	0,00
117177	RAB3IP	RAB3A interacting protein (rab3in3)	0,53	0,02

5914	RARA	retinoic acid receptor, alpha	0,52	0,04
81894	SLC25A28	solute carrier family 25, member 28	0,52	0,03
3158	HMGCS2	3-hydroxy-3-methylglutaryl-Coenzyme A synthase 2 (mitochondrial)	0,52	0,05
8406	SRPX	sushi-repeat-containing protein, X-linked	0,52	0,00
54780	NSMCE4A	non-SMC element 4 homolog A (S. cerevisiae)	0,52	0,00
115123	MARCH3	membrane-associated ring finger (C3HC4) 3	0,52	0,03
58489	FAM108C1	family with sequence similarity 108, member C1	0,51	0,02
84916	CIRH1A	cirrhosis, autosomal recessive 1A (cirhin)	0,51	0,01
140809	SRXN1	sulfiredoxin 1 homolog (S. cerevisiae)	0,50	0,03
80306	MED28	mediator complex subunit 28	0,50	0,03
57630	SH3RF1	SH3 domain containing ring finger 1	0,50	0,01
3700	ITIH4	inter-alpha (globulin) inhibitor H4 (plasma Kallikrein-sensitive glycoprotein)	0,50	0,00
85464	SSH2	slingshot homolog 2 (Drosophila)	0,50	0,01
6774	STAT3	signal transducer and activator of transcription 3 (acute-phase response factor)	0,50	0,02
84940	CORO6	coronin 6	0,49	0,00
79188	TMEM43	transmembrane protein 43	0,49	0,04
4953	ODC1	ornithine decarboxylase 1	0,48	0,04
26959	HBP1	poly(A) binding protein, cytoplasmic pseudogene 5; poly(A) binding protein, cytoplasmic 1	0,48	0,00
5144	PDE4D	phosphodiesterase 4D, cAMP-specific (phosphodiesterase E3 duncce homolog, Drosophila)	0,48	0,00
23013	SPEN	spen homolog, transcriptional regulator (Drosophila)	0,48	0,00
5954	RCN1	reticulocalbin 1, EF-hand calcium binding domain	0,48	0,02
865	CBFB	core-binding factor, beta subunit	0,48	0,00
7048	TGFBR2	transforming growth factor, beta receptor II (70/80kDa)	0,47	0,02
6584	SLC22A5	solute carrier family 22 (organic cation/carnitine transporter), member 5	0,47	0,05
51602	NOP58	NOP58 ribonucleoprotein homolog (yeast)	0,47	0,03
55127	HEATR1	HEAT repeat containing 1	0,47	0,01
54517	PUS7	pseudouridylylate synthase 7 homolog (S. cerevisiae)	0,47	0,02
3099	HK2	hexokinase 2 pseudogene; hexokinase 2	0,47	0,03
10606	PAICS	phosphoribosylaminoimidazole carboxylase, phosphoribosylaminoimidazole succinocarboxamide synthetase	0,47	0,03

4302	MLLT6	myeloid/lymphoid or mixed-lineage leukemia (trithorax homolog, Drosophila); translocated to, 6	0,47	0,01
7052	TGM2	transglutaminase 2 (C polypeptide, protein-glutamine-gamma-glutamyltransferase)	0,46	0,01
8291	DYSF	dysferlin, limb girdle muscular dystrophy 2B (autosomal recessive)	0,46	0,03
3182	HNRNPAB	heterogeneous nuclear ribonucleoprotein A/B	0,46	0,03
684959	SNORA25	TATA box binding protein (TBP)-associated factor, RNA polymerase I, D, 41kDa; small nucleolar RNA, H/ACA box 32; small nucleolar RNA, H/ACA box 25	0,46	0,03
4691	NCL	nucleolin	0,46	0,00
26986	PABPC1	poly(A) binding protein, cytoplasmic pseudogene 5; poly(A) binding protein, cytoplasmic I	0,46	0,04
10528	NOP56	NOP56 ribonucleoprotein homolog (yeast)	0,46	0,01
1912	PHC2	polyhomeotic homolog 2 (Drosophila)	0,46	0,02
50999	TMED5	transmembrane emp24 protein transport domain containing 5	0,45	0,00
1837	DTNA	dystrobrevin, alpha	0,45	0,02
9284	NPIP	nuclear pore complex interacting protein	0,45	0,00
3597	IL13RA1	interleukin 13 receptor, alpha 1	0,45	0,01
9214	FAIM3	Fas apoptotic inhibitory molecule 3	0,45	0,01
10432	RBM14	RNA binding motif protein 14; RNA binding motif protein 4	0,45	0,02
84549	MAK16	MAK16 homolog (S. cerevisiae)	0,45	0,01
10656	KHDRBS3	KH domain containing, RNA binding, signal transduction associated 3	0,45	0,03
7920	BAT5	HLA-B associated transcript 5	0,45	0,00
23558	WBP2	WW domain binding protein 2	0,44	0,00
9933	KIAA0020	KIAA0020	0,44	0,05
9533	POLR1C	polymerase (RNA) I polypeptide C, 30kDa	0,44	0,05
10068	IL18BP	interleukin 18 binding protein	0,44	0,03
26018	LRIG1	acyl-CoA thioesterase 11	0,44	0,02
6780	STAU1	staufen, RNA binding protein, homolog 1 (Drosophila)	0,44	0,01
10079	ATP9A	ATPase, class II, type 9A	0,44	0,02
7050	TGIF1	TGFB-induced factor homeobox 1	0,43	0,03
8204	NRIP1	nuclear receptor interacting protein 1	0,43	0,01
311	ANXA11	annexin A11	0,43	0,02

4790	NFKB1	nuclear factor of kappa light polypeptide gene enhancer in B-cells 1	0,43	0,01
9564	BCAR1	similar to breast cancer anti-estrogen resistance 1; breast cancer anti-estrogen resistance 1	0,43	0,01
54458	PRR13	proline rich 13	0,43	0,01
8408	ULK1	unc-51-like kinase 1 ( <i>C. elegans</i> )	0,43	0,00
4864	NPC1	Niemann-Pick disease, type C1	0,43	0,02
337867	UBAC2	UBA domain containing 2	0,43	0,05
7994	MYST3	MYST histone acetyltransferase (monocytic leukemia) 3	0,43	0,01
6583	SLC22A4	solute carrier family 22 (organic cation/ergothioneine transporter), member 4	0,43	0,01
2531	FVT1	3-ketodihydrophingosine reductase	0,42	0,02
51104	FAM108B1	family with sequence similarity 108, member B1	0,42	0,02
283635	FAM177A1	family with sequence similarity 177, member A1	0,42	0,02
85456	TNKS1BP1	tankyrase 1 binding protein 1, 182kDa	0,42	0,01
4282	MIF	macrophage migration inhibitory factor (glycosylation-inhibiting factor)	0,42	0,00
6059	ABCE1	similar to ATP-binding cassette, sub-family E, member 1; ATP-binding cassette, sub-family E (OABP), member 1	0,42	0,02
55559	UCHL5IP	three prime repair exonuclease 2; HAU5 augmin-like complex, subunit 7	0,42	0,02
3588	IL10RB	interleukin 10 receptor, beta	0,42	0,02
8428	STK24	serine/threonine kinase 24 (STE20 homolog, yeast)	0,42	0,02
29889	GNL2	guanine nucleotide binding protein-like 2 (nucleolar)	0,41	0,01
80820	EEPD1	endonuclease/exonuclease/phosphatase family domain containing 1	0,41	0,01
81631	MAP1LC3B	microtubule-associated protein 1 light chain 3 beta	0,40	0,00
206358	SLC36A1	solute carrier family 36 (proton/amino acid symporter), member 1	0,40	0,01
9354	UBE4A	ubiquitination factor E4A (UFD2 homolog, yeast)	0,40	0,00
79042	TSEN34	tRNA splicing endonuclease 34 homolog ( <i>S. cerevisiae</i> )	0,40	0,00
3964	LGALS8	lectin, galactoside-binding, soluble, 8	0,40	0,01
6780	STAU1	serine/threonine kinase 3 (STE20 homolog, yeast)	0,40	0,01
56940	DUSP22	similar to mitogen-activated protein kinase phosphatase x; dual specificity phosphatase 22	0,40	0,02
3665	IRF7	interferon regulatory factor 7	0,40	0,01
9416	DDX23	DEAD (Asp-Glu-Ala-Asp) box polypeptide 23	0,40	0,00
22863	KIAA0831	KIAA0831	0,39	0,00



4170	MCL1	myeloid cell leukemia sequence 1 (BCL2-related)	0,39	0,01
8819	SAP30	Sin3A-associated protein, 30kDa	0,39	0,00
6507	SLC1A3	solute carrier family 1 (glial high affinity glutamate transporter), member 3	0,39	0,03
3251	HPRT1	hypoxanthine phosphoribosyltransferase 1	0,39	0,00
768211	RELL1	RELT-like 1	0,39	0,03
9589	WTAP	Wilms tumor 1 associated protein	0,39	0,01
4839	NOP2	NOP2 nucleolar protein homolog (yeast)	0,39	0,02
124402	FAM100A	family with sequence similarity 100, member A	0,38	0,01
4673	NAP1L1	nucleosome assembly protein 1-like 1	0,38	0,01
83719	YPEL3	yippee-like 3 (Drosophila)	0,38	0,00
26094	WDR21A	ribosomal L1 domain containing 1	0,38	0,00
9991	ROD1	ROD1 regulator of differentiation 1 ( <i>S. pombe</i> )	0,38	0,03
64718	UNKL	unkempt homolog (Drosophila)-like	0,38	0,00
57700	FAM160B1	family with sequence similarity 160, member B1	0,38	0,00
1736	DKC1	dyskeratosis congenita 1, dyskerin	0,38	0,05
54915	YTHDF1	YTH domain family, member 1	0,38	0,04
1454	CSNK1E	casein kinase 1, epsilon	0,38	0,00
3148	HMGB2	high-mobility group box 2	0,38	0,00
6675	UAPI	UDP-N-acetylglucosamine pyrophosphorylase 1	0,37	0,04
56902	PNO1	partner of NOB1 homolog ( <i>S. cerevisiae</i> )	0,37	0,02
780	DDR1	discoidin domain receptor tyrosine kinase 1	0,37	0,00
5718	PSMD12	proteasome (prosome, macropain) 26S subunit, non-ATPase, 12	0,37	0,01
23531	MMD	monocyte to macrophage differentiation-associated	0,37	0,00
29121	CLEC2D	C-type lectin domain family 2, member D	0,37	0,00
79693	YRDC	yrdC domain containing ( <i>E. coli</i> )	0,37	0,02
81929	SEH1L	SEH1-like ( <i>S. cerevisiae</i> )	0,37	0,04
5036	PA2G4	proliferation-associated 2G4, 38kDa; proliferation-associated 2G4 pseudogene 4	0,37	0,01
5905	RANGAP1	Ran GTPase activating protein 1	0,37	0,04
9961	MVP	major vault protein	0,37	0,03
9332	CD163	CD163 molecule	0,37	0,02

135293	PM20D2	peptidase M20 domain containing 2	0,37	0,00
114907	FBXO32	F-box protein 32	0,37	0,01
25829	TMEM184B	ASF1 anti-silencing function 1 homolog A ( <i>S. cerevisiae</i> )	0,37	0,02
2274	FHL2	four and a half LIM domains 2	0,37	0,02
5175	PECAM1	platelet/endothelial cell adhesion molecule	0,36	0,04
26258	PLDN	F-box protein 10	0,36	0,04
113791	PIK3IP1	major facilitator superfamily domain containing 3	0,36	0,04
65979	PHACTR4	phosphatase and actin regulator 4	0,36	0,04
121260	SLC15A4	solute carrier family 15, member 4	0,36	0,01
378805	FLJ43663	hypothetical LOC378805	0,36	0,01
84248	FYTTDI	forty-two-three domain containing 1	0,36	0,02
54663	WDR74	WD repeat domain 74	0,36	0,01
83743	GRWD1	glutamate-rich WD repeat containing 1	0,36	0,02
9057	SLC7A6	solute carrier family 7 (cationic amino acid transporter, y <sup>+</sup> system), member 6	0,36	0,00
10768	AHCYL1	adenosylhomocysteinase-like 1	0,36	0,01
29799	YPEL1	yippee-like 1 ( <i>Drosophila</i> )	0,36	0,01
129303	TMEM150A	transmembrane protein 150A	0,36	0,00
3570	IL6R	interleukin 6 receptor	0,36	0,01
10758	TRAF3IP2	TRAF3 interacting protein 2	0,36	0,01
7705	ZNF146	zinc finger protein 146	0,35	0,04
57178	ZMIZ1	zinc finger, MIZ-type containing 1	0,35	0,00
715	C1R	complement component 1, r subcomponent	0,35	0,05
54432	YIPF1	Yip1 domain family, member 1	0,35	0,00
10777	ARPP-21	cyclic AMP-regulated phosphoprotein, 21 kD	0,35	0,02
3615	IMPDH2	IMP (inosine monophosphate) dehydrogenase 2	0,35	0,02
10144	FAM13A	family with sequence similarity 13, member A	0,35	0,02
6950	TCPI	hypothetical gene supported by BC000665; t-complex 1	0,35	0,01
59338	PLEKHA1	pleckstrin homology domain containing, family A (phosphoinositide binding specific) member 1	0,35	0,05
83666	PARP9	poly (ADP-ribose) polymerase family, member 9	0,35	0,00

1017	CDK2		cyclin-dependent kinase 2	0,35	0,03
8882	ZNF259		zinc finger protein 259	0,35	0,01
79791	FBXO31		F-box protein 31	0,35	0,00
55646	LYAR		Ly1 antibody reactive homolog (mouse)	0,34	0,05
81603	TRIM8		tripartite motif-containing 8	0,34	0,00
10196	PRMT3		protein arginine methyltransferase 3	0,34	0,01
6009	RHEB		Ras homolog enriched in brain	0,34	0,03
57169	ZNFX1		zinc finger, NFX1-type containing 1	0,34	0,00
4927	NUP88		nucleoporin 88kDa	0,34	0,00
137492	VPS37A		vacuolar protein sorting 37 homolog A ( <i>S. cerevisiae</i> )	0,34	0,03
8312	AXIN1		axin 1	0,34	0,00
8613	PPAP2B		phosphatidic acid phosphatase type 2B	0,34	0,01
8890	EIF2B4		eukaryotic translation initiation factor 2B, subunit 4 delta, 67kDa	0,34	0,02
8624	PSMG1		proteasome (prosome, macropain) assembly chaperone 1	0,34	0,02
23560	GTPBP4		GTP binding protein 4	0,34	0,05
57658	CALCOCO1		calcium binding and coiled-coil domain 1	0,34	0,00
187	APLNR		apelin receptor	0,34	0,00
84640	USP38		ubiquitin specific peptidase 38	0,34	0,01
2618	GART		phosphoribosylglycinamide formyltransferase, phosphoribosylglycinamide synthetase, phosphoribosylaminoimidazole synthetase	0,33	0,01
6229	RPS24		ribosomal protein S24	0,33	0,04
7844	RNF103		vacuolar protein sorting 24 homolog ( <i>S. cerevisiae</i> ); ring finger protein 103	0,33	0,01
10509	SEMA4B		sema domain, immunoglobulin domain (Ig), transmembrane domain (TM) and short cytoplasmic domain, (semaphorin) 4B	0,33	0,04
140885	SIRPA		signal-regulatory protein alpha	0,33	0,02
22926	ATF6		activating transcription factor 6	0,33	0,03
4008	LMO7		LIM domain 7	0,33	0,00
8824	CES2		carboxylesterase 2 (intestine, liver)	0,33	0,01
140890	SFRS12		splicing factor, arginine/serine-rich 12	0,33	0,00
23253	ANKRD12		ankyrin repeat domain 12	0,33	0,01

55810	FOXJ2	forkhead box J2	0,33	0,04
84085	FBXO30	F-box protein 30	0,33	0,00
54935	DUSP23	dual specificity phosphatase 23	0,33	0,05
3675	ITGA3	integrin, alpha 3 (antigen CD49C, alpha 3 subunit of VLA-3 receptor)	0,32	0,01
138428	PTRH1	peptidyl-tRNA hydrolase 1 homolog ( <i>S. cerevisiae</i> )	0,32	0,04
27075	TSPAN13	tetraspanin 13	0,32	0,02
7528	YY1	YY1 transcription factor	0,32	0,00
80135	RPF1	brix domain containing 5	0,32	0,00
51678	MPP6	membrane protein, palmitoylated 6 (MAGUK p55 subfamily member 6)	0,32	0,00
114882	OSBPL8	oxysterol binding protein-like 8	0,32	0,00
80216	ALPK1	alpha-kinase 1	0,32	0,00
29110	TBK1	TANK-binding kinase 1	0,32	0,00
25996	REXO2	leucine-rich repeats and immunoglobulin-like domains 1	0,32	0,01
1116	CHI3L1	chitinase 3-like 1 (cartilage glycoprotein-39)	0,31	0,04
91	ACVR1B	activin A receptor, type IB	0,31	0,02
4097	MAFG	v-maf musculoaponeurotic fibrosarcoma oncogene homolog G (avian)	0,31	0,00
1942	EFNA1	ephrin-A1	0,31	0,01
54675	CRLS1	cardiolipin synthase 1	0,31	0,01
157697	ERICHI	glutamate-rich 1	0,31	0,01
343990	MGC42367	chromosome 2 open reading frame 55	0,31	0,03
4666	NACA	nascent polypeptide-associated complex alpha subunit	0,31	0,01
3790	KCNS3	potassium voltage-gated channel, delayed-rectifier, subfamily S, member 3	0,31	0,02
26156	RSL1D1	pallidin homolog (mouse)	0,31	0,00
1665	DHX15	DEAH (Asp-Glu-Ala-His) box polypeptide 15	0,31	0,02
6520	SLC3A2	solute carrier family 3 (activators of dibasic and neutral amino acid transport), member 2	0,31	0,02
64393	ZMAT3	zinc finger, matrin type 3	0,31	0,01
9727	RAB11FIP3	RAB11 family interacting protein 3 (class II)	0,31	0,04
22880	MORC2	MORC family CW-type zinc finger 2	0,30	0,01
54707	GPN2	GPN-loop GTPase 2	0,30	0,04
6710	SPTB	spectrin, beta, erythrocytic	0,30	0,01

9972	NUP153	nucleoporin 153kDa	0,30	0,01
259217	HSPA12A	heat shock 70kDa protein 12A	0,30	0,02
63876	PKNOX2	PBX/knotted 1 homeobox 2	0,30	0,02
83593	RASSF5	Ras association (RalGDS/AF-6) domain family member 5	0,30	0,03
4779	NFE2L1	nuclear factor (erythroid-derived 2)-like 1	0,30	0,02
23411	SIRT1	sirtuin (silent mating type information regulation 2 homolog) 1 ( <i>S. cerevisiae</i> )	0,30	0,01
84128	WDR75	WD repeat domain 75	0,30	0,01
135112	NCOA7	nuclear receptor coactivator 7	0,30	0,02
29097	CNIH4	cornichon homolog 4 ( <i>Drosophila</i> )	0,30	0,02
85358	SHANK3	SH3 and multiple ankyrin repeat domains 3	0,30	0,01
9988	DMTF1	cyclin D binding myb-like transcription factor 1	0,30	0,02
90850	ZNF598	zinc finger protein 598	0,30	0,02
55205	ZNF532	similar to zinc finger protein 347; zinc finger protein 532	0,29	0,02
88455	ANKRD13A	ankyrin repeat domain 13A	0,29	0,02
56919	DHX33	DEAH (Asp-Glu-Ala-His) box polypeptide 33	0,29	0,05
51010	EXOSC3	exosome component 3	0,29	0,03
4286	MITF	microphthalmia-associated transcription factor	0,29	0,02
51283	BFAR	bifunctional apoptosis regulator	0,29	0,02
5757	PTMA	hypothetical LOC728026; prothymosin, alpha; hypothetical gene supported by BC013859; prothymosin, alpha pseudogene 4 (gene sequence 112)	0,29	0,01
50640	PNPLA8	patatin-like phospholipase domain containing 8	0,29	0,03
5936	RBM4	RNA binding motif protein 14; RNA binding motif protein 4	0,29	0,02
285704	RGMB	RGM domain family, member B	0,29	0,01
3431	SPI10	SPI10 nuclear body protein	0,29	0,01
10964	IFI44L	interferon-induced protein 44-like	0,29	0,01
55718	POLR3E	polymerase (RNA) III (DNA directed) polypeptide E (80kD)	0,29	0,01
9766	KIAA0247	KIAA0247	0,29	0,03
79733	E2F8	E2F transcription factor 8	0,29	0,03
1464	CSPG4	chondroitin sulfate proteoglycan 4	0,29	0,02
2028	ENPEP	glutamyl aminopeptidase (aminopeptidase A)	0,28	0,05

23177	CEP68	centrosomal protein 68kDa	0,28	0,01
26511	CHIC2	olfactory receptor, family 7, subfamily E, member 37 pseudogene	0,28	0,02
57510	XPO5	exportin 5	0,28	0,01
5478	PPIA	similar to TRIMCyp; peptidylprolyl isomerase A (cyclophilin A); peptidylprolyl isomerase A (cyclophilin A)-like 3	0,28	0,01
84171	LOXL4	lysyl oxidase-like 4	0,28	0,02
84312	BRMS1L	breast cancer metastasis-suppressor 1-like	0,28	0,00
6310	ATXN1	ataxin 1	0,28	0,01
56984	PSMG2	proteasome (prosome, macropain) assembly chaperone 2	0,28	0,00
25942	SIN3A	dehydrogenase/reductase (SDR family) member 7B	0,28	0,01
6777	STAT5B	signal transducer and activator of transcription 5B	0,28	0,05
9718	ECE2	endothelin converting enzyme 2	0,28	0,02
23011	RAB21	RAB21, member RAS oncogene family	0,28	0,01
81567	TXNDC5	thioredoxin domain containing 5 (endoplasmic reticulum); muted homolog (mouse)	0,28	0,01
29954	POMT2	protein-O-mannosyltransferase 2	0,28	0,01
25778	DSTYK	dual serine/threonine and tyrosine protein kinase	0,28	0,01
51082	POLR1D	polymerase (RNA) I polypeptide D, 16kDa	0,28	0,00
8662	EIF3B	eukaryotic translation initiation factor 3, subunit B	0,27	0,04
677	ZFP36L1	zinc finger protein 36, C3H type-like 1	0,27	0,01
8473	OGT	O-linked N-acetylglucosamine (GlcNAc) transferase (UDP-N-acetylglucosamine:polypeptide-N-acetylglucosaminyl transferase)	0,27	0,00
9180	OSMR	oncostatin M receptor	0,27	0,05
84665	MYPN	myopalladin	0,27	0,05
191	AHCY	adenosylhomocysteinase	0,27	0,01
84864	MINA	MYC induced nuclear antigen	0,27	0,03
6788	STK3	aurora kinase A; aurora kinase A pseudogene 1	0,27	0,02
3620	INDO	indoleamine 2,3-dioxygenase 1	0,27	0,03
9043	SPAG9	sperm associated antigen 9	0,27	0,02
54881	TEX10	testis expressed 10	0,27	0,01
6772	STAT1	signal transducer and activator of transcription 1, 91kDa	0,27	0,01

27309	ZNF330	zinc finger protein 330	0,27	0,00
57685	CACHD1	cache domain containing 1	0,27	0,03
1362	CPD	carboxypeptidase D	0,27	0,00
9911	TMCC2	transmembrane and coiled-coil domain family 2	0,27	0,01
51315	KRCC1	lysine-rich coiled-coil 1	0,27	0,01
79139	DERL1	Der1-like domain family, member 1	0,26	0,01
7005	TEAD3	TEA domain family member 3	0,26	0,03
84918	LRP11	low density lipoprotein receptor-related protein 11	0,26	0,00
272	AMPD3	adenosine monophosphate deaminase (isoform E)	0,26	0,00
10597	TRAPPC2P1	trafficking protein particle complex 2; trafficking protein particle complex 2 pseudogene 1	0,26	0,04
5937	RBMS1	RNA binding motif, single stranded interacting protein 1	0,26	0,03
5516	PPP2CB	protein phosphatase 2 (formerly 2A), catalytic subunit, beta isoform	0,26	0,03
2104	ESRRG	estrogen-related receptor gamma	0,26	0,00
92912	UBE2Q2	ubiquitin-conjugating enzyme E2Q family member 2	0,26	0,03
55800	SCN3B	sodium channel, voltage-gated, type III, beta	0,26	0,01
63893	UBE2O	ubiquitin-conjugating enzyme E2O	0,26	0,01
80325	ABTB1	ankyrin repeat and BTB (POZ) domain containing 1	0,26	0,02
55813	UTP6	UTP6, small subunit (SSU) processome component, homolog (yeast)	0,26	0,01
10952	SEC61B	Sec61 beta subunit	0,26	0,04
114793	FMNL2	formin-like 2	0,26	0,05
57664	PLEKHA4	pleckstrin homology domain containing, family A (phosphoinositide binding specific) member 4	0,26	0,04
83787	ARMC10	armadillo repeat containing 10	0,26	0,04
23214	XPO6	exportin 6	0,26	0,03
3066	HDAC2	histone deacetylase 2	0,26	0,01
51065	RPS27L	ribosomal protein S27-like	0,26	0,04
64782	AEN	apoptosis enhancing nuclease	0,26	0,03
55207	ARL8B	ADP-ribosylation factor-like 8B	0,26	0,03
535	ATP6V0A1	ATPase, H+ transporting, lysosomal V0 subunit a1	0,25	0,03
11091	WDR5	WD repeat domain 5	0,25	0,01

58490	RPRD1B	regulation of nuclear pre-mRNA domain containing 1B	0,25	0,01
114908	TMEM123	transmembrane protein 123	0,25	0,00
51056	LAP3	leucine aminopeptidase 3	0,25	0,04
55349	CHDH	choline dehydrogenase	0,25	0,00
831	CAST	calpastatin	0,25	0,03
10865	ARID5A	AT rich interactive domain 5A (MRF1-like)	0,25	0,00
6840	SVIL	supervillin	0,25	0,02
817	CAMK2D	calcium/calmodulin-dependent protein kinase II delta	0,25	0,01
2752	GLUL	glutamate-ammonia ligase (glutamine synthetase)	0,25	0,04
3189	HNRPH3	heterogeneous nuclear ribonucleoprotein H3 (ZH9)	0,25	0,03
10436	EMG1	EMG1 nucleolar protein homolog (S. cerevisiae)	0,25	0,04
6103	RPGR	retinitis pigmentosa GTPase regulator	0,25	0,01
23162	MAPK8IP3	mitogen-activated protein kinase 8 interacting protein 3	0,25	0,00
10413	YAP1	Yes-associated protein 1, 65kDa	0,25	0,05
31	ACACA	acetyl-Coenzyme A carboxylase alpha	0,25	0,00
2665	GDI2	GDP dissociation inhibitor 2	0,25	0,03
4430	MYO1B	myosin IB	0,25	0,05
5887	RAD23B	RAD23 homolog B (S. cerevisiae)	0,25	0,05
25825	BACE2	transmembrane protein 184B	0,25	0,02
10199	MPHOSPH10	M-phase phosphoprotein 10 (U3 small nucleolar ribonucleoprotein)	0,25	0,03
23392	KIAA0368	KIAA0368	0,25	0,04
54464	XRN1	5'-3' exoribonuclease 1	0,25	0,01
10782	ZNF274	zinc finger protein 274	0,25	0,02
54865	GPATCH4	G patch domain containing 4	0,25	0,03
25778	RIPK5	RAS guanyl releasing protein 3 (calcium and DAG-regulated)	0,25	0,03
64951	MRPS24	mitochondrial ribosomal protein S24	-0,25	0,04
9491	PSMF1	proteasome (prosome, macropain) inhibitor subunit 1 (PI31)	-0,25	0,00
5787	PTPRB	protein tyrosine phosphatase, receptor type, B	-0,25	0,02
8087	FXR1	fragile X mental retardation, autosomal homolog 1	-0,25	0,03
22913	RALY	RNA binding protein, autoantigenic (hnRNP-associated with lethal yellow homolog	-0,25	0,02



		(mouse))			
<b>122622</b>	ADSSL1	adenylosuccinate synthase like 1		-0,25	0,00
<b>6687</b>	SPG7	spastic paraplegia 7 (pure and complicated autosomal recessive)		-0,25	0,02
<b>1512</b>	CTSH	cathepsin H		-0,25	0,00
<b>114876</b>	OSBPL1A	oxysterol binding protein-like 1A		-0,25	0,03
<b>92106</b>	MGC15763	oxidoreductase NAD-binding domain containing 1		-0,25	0,01
<b>6549</b>	SLC9A2	solute carrier family 9 (sodium/hydrogen exchanger), member 2		-0,25	0,01
<b>6563</b>	SLC14A1	solute carrier family 14 (urea transporter), member 1 (Kidd blood group)		-0,25	0,01
<b>339123</b>	JMJD8	jumonji domain containing 8		-0,25	0,03
<b>29911</b>	HOOK2	hook homolog 2 (Drosophila)		-0,25	0,01
<b>10138</b>	YAF2	YY1 associated factor 2		-0,25	0,02
<b>55788</b>	LMBRD1	LMBR1 domain containing 1		-0,25	0,03
<b>79077</b>	DC TPP1	dCTP pyrophosphatase 1		-0,25	0,04
<b>92259</b>	MRPS36	mitochondrial ribosomal protein S36		-0,25	0,02
<b>79894</b>	ZNF672	zinc finger protein 672; hypothetical LOC100130262		-0,25	0,03
<b>55755</b>	CDK5RAP2	CDK5 regulatory subunit associated protein 2		-0,25	0,03
<b>389257</b>	LRRC14B	leucine-rich repeat-containing protein 14-like		-0,25	0,03
<b>498</b>	ATP5A1	ATP synthase, H+ transporting, mitochondrial F1 complex, alpha subunit 1, cardiac muscle		-0,25	0,01
<b>5250</b>	SLC25A3	solute carrier family 25 (mitochondrial carrier; phosphate carrier), member 3		-0,25	0,01
<b>126306</b>	JSRP1	junctional sarcoplasmic reticulum protein 1		-0,25	0,00
<b>374291</b>	NDUFS7	NADH dehydrogenase (ubiquinone) Fe-S protein 7, 20kDa (NADH-coenzyme Q reductase)		-0,25	0,01
<b>9604</b>	RNF14	ring finger protein 14		-0,25	0,02
<b>253738</b>	EBF3	early B-cell factor 3		-0,25	0,03
<b>64285</b>	RHBDF1	rhomboid 5 homolog 1 (Drosophila)		-0,25	0,01
<b>54205</b>	CYCS	cytochrome c, somatic		-0,25	0,01
<b>139285</b>	FLJ39827	family with sequence similarity 123B		-0,25	0,03
<b>118472</b>	ZNF511	zinc finger protein 511		-0,25	0,02
<b>6237</b>	RRAS	related RAS viral (r-ras) oncogene homolog		-0,25	0,01
<b>51530</b>	ZC3HC1	zinc finger, C3HC-type containing 1		-0,26	0,01

4802	NFYC	nuclear transcription factor Y, gamma	-0,26	0,01
55486	PARL	presenilin associated, rhomboid-like	-0,26	0,00
5583	PRKCH	protein kinase C, eta	-0,26	0,02
9552	SPAG7	sperm associated antigen 7	-0,26	0,00
219749	ZNF25	zinc finger protein 25	-0,26	0,00
53826	FXYD6	FXYD domain containing ion transport regulator 6	-0,26	0,01
7867	MAPKAPK3	mitogen-activated protein kinase-activated protein kinase 3	-0,26	0,01
6596	HLTF	helicase-like transcription factor	-0,26	0,03
90624	LYRM7	Lyrm7 homolog (mouse)	-0,26	0,04
112724	RDH13	retinol dehydrogenase 13 (all-trans/9-cis)	-0,26	0,02
8605	PLA2G4C	phospholipase A2, group IVC (cytosolic, calcium-independent)	-0,26	0,02
55052	MRPL20	similar to mitochondrial ribosomal protein L20; mitochondrial ribosomal protein L20	-0,26	0,01
3312	HSPA8	heat shock 70kDa protein 8	-0,26	0,02
22921	MSRB2	methionine sulfoxide reductase B2	-0,26	0,01
26827	RNU6-1	5-oxoprolinase (ATP-hydrolysing)	-0,26	0,02
26275	HIBCH	guanine nucleotide binding protein-like 3 (nucleolar)	-0,26	0,02
10817	FRS3	fibroblast growth factor receptor substrate 3	-0,26	0,01
26508	HEYL	cysteine-rich hydrophobic domain 2	-0,26	0,01
54795	TRPM4	transient receptor potential cation channel, subfamily M, member 4	-0,26	0,04
5296	PIK3R2	phosphoinositide-3-kinase, regulatory subunit 2 (beta)	-0,27	0,02
9781	RNF144	ring finger protein 144A	-0,27	0,01
529	ATP6V1E1	ATPase, H+ transporting, lysosomal 31kDa, V1 subunit E1	-0,27	0,05
1163	CKS1B	CDC28 protein kinase regulatory subunit 1B	-0,27	0,00
51016	FAM158A	family with sequence similarity 158, member A	-0,27	0,01
28958	CCDC56	coiled-coil domain containing 56	-0,27	0,00
7956	ERMP1	endoplasmic reticulum metalloproteinase 1	-0,27	0,01
26636	OR7E37P	RNA, U6 small nuclear 2; RNA, U6 small nuclear 1	-0,27	0,01
10099	TSPAN3	tetraspanin 3	-0,27	0,01
79005	SCNM1	sodium channel modifier 1	-0,27	0,01
7169	TPM2	tropomyosin 2 (beta)	-0,27	0,02

10890	RAB10	RAB10, member RAS oncogene family	-0,27	0,01
81618	ITM2C	integral membrane protein 2C	-0,27	0,01
57153	SLC44A2	solute carrier family 44, member 2	-0,27	0,03
55745	MUDENG	MU-2/AP1M2 domain containing, death-inducing	-0,27	0,02
1355	COX15	COX15 homolog, cytochrome c oxidase assembly protein (yeast)	-0,27	0,00
23553	HYAL4	hyaluronoglucosaminidase 4	-0,27	0,03
285193	DUSP28	dual specificity phosphatase 28	-0,27	0,03
5699	PSMB10	proteasome (prosome, macropain) subunit, beta type, 10	-0,27	0,01
5358	PLS3	plastin 3 (T isoform)	-0,27	0,03
51075	TXNDC14	thioredoxin-related transmembrane protein 2	-0,27	0,00
10295	BCKDK	branched chain ketoacid dehydrogenase kinase	-0,27	0,03
1593	CYP27A1	cytochrome P450, family 27, subfamily A, polypeptide 1	-0,27	0,05
516	ATP5G1	ATP synthase, H+ transporting, mitochondrial F0 complex, subunit C1 (subunit 9)	-0,28	0,03
523	ATP6V1A	ATPase, H+ transporting, lysosomal 70kDa, V1 subunit A	-0,28	0,02
5524	PPP2R4	protein phosphatase 2A activator, regulatory subunit 4	-0,28	0,00
4005	LMO2	LIM domain only 2 (rhototin-like 1)	-0,28	0,01
1352	COX10	COX10 homolog, cytochrome c oxidase assembly protein, heme A: farnesyltransferase (yeast)	-0,28	0,00
6242	RTKN	rhotekin	-0,28	0,00
57107	PDSS2	prenyl (decaprenyl) diphosphate synthase, subunit 2	-0,28	0,00
2021	ENDOG	endonuclease G	-0,28	0,00
123169	LEO1	Leo1, Paf1/RNA polymerase II complex component, homolog ( <i>S. cerevisiae</i> )	-0,28	0,00
55347	ABHD10	abhydrolase domain containing 10	-0,28	0,02
147184	TMEM99	transmembrane protein 99	-0,28	0,04
51734	SEPX1	selenoprotein X, 1	-0,28	0,01
3385	ICAM3	intercellular adhesion molecule 3	-0,28	0,01
2882	GPX7	glutathione peroxidase 7	-0,28	0,05
952	CD38	CD38 molecule	-0,28	0,03
858	CAV2	caveolin 2	-0,28	0,05
6482	ST3GAL1	ST3 beta-galactoside alpha-2,3-sialyltransferase 1	-0,28	0,05

7390	UROS	uroporphyrinogen III synthase	-0,28	0,01
5859	QARS	glutamyl-tRNA synthetase	-0,28	0,01
84816	RTN4IP1	reticulon 4 interacting protein 1	-0,29	0,00
169611	OLFML2A	olfactomedin-like 2A	-0,29	0,02
360132	FKBP9L	FK506 binding protein 9-like	-0,29	0,04
57060	PCBP4	poly(rC) binding protein 4	-0,29	0,01
23446	SLC44A1	solute carrier family 44, member 1	-0,29	0,00
4856	NOV	nephroblastoma overexpressed gene	-0,29	0,03
51455	REV1	REV1 homolog (S. cerevisiae)	-0,29	0,01
80207	OPA3	optic atrophy 3 (autosomal recessive, with chorea and spastic paraplegia)	-0,29	0,03
5210	PFKFB4	6-phosphofructo-2-kinase/fructose-2,6-biphosphatase 4	-0,29	0,02
64975	MRPL41	mitochondrial ribosomal protein L41	-0,29	0,04
155066	ATP6V0E2	ATPase, H+ transporting V0 subunit e2	-0,29	0,01
2592	GALT	galactose-1-phosphate uridylyltransferase	-0,29	0,04
79135	APOO	apolipoprotein O	-0,29	0,01
29074	MRPL18	mitochondrial ribosomal protein L18	-0,29	0,01
90313	TP53I13	tumor protein p53 inducible protein 13	-0,29	0,00
522	ATP5J	ATP synthase, H+ transporting, mitochondrial F0 complex, subunit F6	-0,29	0,04
29928	TIMM22	translocase of inner mitochondrial membrane 22 homolog (yeast)	-0,29	0,00
6100	RP9	retinitis pigmentosa 9 (autosomal dominant)	-0,29	0,01
55852	TEX2	testis expressed 2	-0,29	0,05
51069	MRPL2	mitochondrial ribosomal protein L2	-0,29	0,02
23187	PHLDB1	pleckstrin homology-like domain, family B, member 1	-0,30	0,01
1632	DCI	dodecenoyl-Coenzyme A delta isomerase (3,2 trans-enoyl-Coenzyme A isomerase)	-0,30	0,02
7263	TST	thiosulfate sulfurtransferase (rhodanese)	-0,30	0,03
3337	DNAJB1	DnaJ (Hsp40) homolog, subfamily B, member 1	-0,30	0,05
369	ARAF	v-raf murine sarcoma 3611 viral oncogene homolog	-0,30	0,03
9717	SEC14L5	SEC14-like 5 (S. cerevisiae)	-0,30	0,03
84967	LSM10	LSM10, U7 small nuclear RNA associated	-0,30	0,01
5420	PODXL	podocalyxin-like	-0,30	0,03

11344	TWF2	twinfilin, actin-binding protein, homolog 2 (Drosophila)	-0,30	0,05
201140	DHRS7C	dehydrogenase/reductase (SDR family) member 7C	-0,30	0,00
5207	PFKFB1	6-phosphofructo-2-kinase/fructose-2,6-biphosphatase 1	-0,30	0,00
23294	ANKS1A	ankyrin repeat and sterile alpha motif domain containing 1A	-0,30	0,02
7079	TIMP4	TIMP metalloproteinase inhibitor 4	-0,30	0,02
55186	SLC25A36	solute carrier family 25, member 36	-0,30	0,04
8869	ST3GAL5	ST3 beta-galactoside alpha-2,3-sialyltransferase 5	-0,30	0,00
140456	ASB11	ankyrin repeat and SOCS box-containing 11	-0,30	0,05
6697	SPR	sepiapterin reductase (7,8-dihydrobiopterin:NADP+ oxidoreductase)	-0,30	0,01
3280	HES1	hairy and enhancer of split 1, (Drosophila)	-0,30	0,02
25979	DHRS7B	REX2, RNA exonuclease 2 homolog (S. cerevisiae)	-0,30	0,01
29803	REPIN1	replication initiator 1	-0,30	0,02
84266	ALKBH7	alkB, alkylation repair homolog 7 (E. coli)	-0,30	0,01
10651	MTX2	metaxin 2	-0,30	0,01
29089	UBE2T	ubiquitin-conjugating enzyme E2T (putative)	-0,30	0,01
51004	COQ6	coenzyme Q6 homolog, monooxygenase (S. cerevisiae)	-0,30	0,01
4713	NDUFB7	NADH dehydrogenase (ubiquinone) 1 beta subcomplex, 7, 18kDa	-0,30	0,00
3858	KRT10	keratin 10	-0,30	0,00
65009	NDRG4	NDRG family member 4	-0,30	0,00
56963	RGMA	RGM domain family, member A	-0,30	0,04
23051	ZHX3	zinc fingers and homeoboxes 3	-0,31	0,03
79675	FASTKD1	FAST kinase domains 1	-0,31	0,01
57048	PLSCR3	phospholipid scramblase 3	-0,31	0,00
23543	RBM9	RNA binding motif protein 9	-0,31	0,03
22911	WDR47	WD repeat domain 47	-0,31	0,02
157310	PEBP4	phosphatidylethanolamine-binding protein 4	-0,31	0,02
8214	DGCR6	DiGeorge syndrome critical region gene 6	-0,31	0,01
112464	PRKCDBP	protein kinase C, delta binding protein	-0,31	0,04
79944	L2HGDH	L-2-hydroxyglutarate dehydrogenase	-0,31	0,00
5201	PFDN1	prefoldin subunit 1	-0,31	0,02

1347	COX7A2	cytochrome c oxidase subunit VIIa polypeptide 2 (liver)	-0,31	0,02
56937	PMEPA1	prostate transmembrane protein, androgen induced 1	-0,31	0,01
4594	MUT	methylmalonyl Coenzyme A mutase	-0,31	0,04
51728	POLR3K	polymerase (RNA) III (DNA directed) polypeptide K, 12.3 kDa	-0,31	0,00
51070	NOSIP	nitric oxide synthase interacting protein	-0,31	0,05
4728	NDUFS8	NADH dehydrogenase (ubiquinone) Fe-S protein 8, 23kDa (NADH-coenzyme Q reductase)	-0,31	0,00
7172	TPMT	thiopurine S-methyltransferase	-0,31	0,01
55268	ECHDC2	enoyl Coenzyme A hydratase domain containing 2	-0,31	0,04
338599	DUPD1	dual specificity phosphatase and pro isomerase domain containing 1	-0,31	0,00
26504	CNNM4	hairy/enhancer-of-split related with YRPW motif-like	-0,31	0,01
55508	SLC35E3	solute carrier family 35, member E3	-0,31	0,02
66000	TMEM108	transmembrane protein 108	-0,31	0,00
54749	EPDR1	ependymin related protein 1 (zebrafish)	-0,31	0,05
404093	CUEDC1	CUE domain containing 1	-0,31	0,02
727956	SDHAP2	succinate dehydrogenase complex, subunit A, flavoprotein pseudogene 2	-0,32	0,01
5789	PTPRD	protein tyrosine phosphatase, receptor type, D	-0,32	0,00
80144	FRAS1	Fraser syndrome 1	-0,32	0,01
51106	TFB1M	transcription factor B1, mitochondrial	-0,32	0,00
64710	NUCKS1	nuclear casein kinase and cyclin-dependent kinase substrate 1	-0,32	0,02
203	AK1	adenylate kinase 1	-0,32	0,05
51334	PRR16	proline rich 16	-0,32	0,00
9612	NCOR2	nuclear receptor co-repressor 2	-0,32	0,04
122786	FRMD6	FERM domain containing 6	-0,32	0,01
6558	SLC12A2	solute carrier family 12 (sodium/potassium/chloride transporters), member 2	-0,32	0,02
255812	SDHALP1	succinate dehydrogenase complex, subunit A, flavoprotein pseudogene 1	-0,32	0,04
8266	UBL4A	ubiquitin-like 4A	-0,32	0,01
154091	SLC2A12	solute carrier family 2 (facilitated glucose transporter), member 12	-0,32	0,01
339344	MYPOP	Myb-related transcription factor, partner of profilin	-0,32	0,01
3157	HMGCS1	3-hydroxy-3-methylglutaryl-Coenzyme A synthase 1 (soluble)	-0,32	0,00

57146	TMEM159	transmembrane protein 159	-0,32	0,03
8635	RNASET2	ribonuclease T2	-0,32	0,03
8604	SLC25A12	solute carrier family 25 (mitochondrial carrier, Aralar), member 12	-0,32	0,04
252995	FNDC5	fibronectin type III domain containing 5	-0,32	0,00
10217	CTDSPL	CTD (carboxy-terminal domain, RNA polymerase II, polypeptide A) small phosphatase-like	-0,32	0,01
27101	CACYBP	similar to calcyclin binding protein; calcyclin binding protein	-0,32	0,01
55090	MED9	mediator complex subunit 9	-0,32	0,01
8404	SPARCL1	SPARC-like 1 (hevin)	-0,32	0,03
65010	SLC26A6	solute carrier family 26, member 6; cadherin, EGF LAG seven-pass G-type receptor 3 (flamingo homolog, Drosophila)	-0,32	0,02
1070	CETN3	centrin, EF-hand protein, 3 (CDC31 homolog, yeast)	-0,33	0,00
9586	CREB5	cAMP responsive element binding protein 5	-0,33	0,00
491	ATP2B2	ATPase, Ca <sup>++</sup> transporting, plasma membrane 2	-0,33	0,01
201164	PLD6	phospholipase D family, member 6	-0,33	0,01
3927	LASP1	LIM and SH3 protein 1	-0,33	0,03
3145	HMBS	hydroxymethylbilane synthase	-0,33	0,01
80212	CCDC92	coiled-coil domain containing 92	-0,33	0,00
388650	FAM69A	family with sequence similarity 69, member A	-0,33	0,00
55168	MRPS18A	mitochondrial ribosomal protein S18A	-0,33	0,00
91687	CENPL	centromere protein L	-0,33	0,03
9452	ITM2A	integral membrane protein 2A	-0,33	0,04
8925	HERC1	hect (homologous to the E6-AP (UBE3A) carboxyl terminus) domain and RCC1 (CHC1)-like domain (RLD) 1	-0,33	0,01
348093	RBPM52	RNA binding protein with multiple splicing 2	-0,33	0,00
65003	MRPL11	mitochondrial ribosomal protein L11	-0,33	0,01
286140	RNF5P1	ring finger protein 5; ring finger protein 5 pseudogene 1	-0,33	0,00
22809	ATF5	activating transcription factor 5	-0,33	0,00
844	CASQ1	calsequestrin 1 (fast-twitch, skeletal muscle)	-0,33	0,00
79844	ZDHC11	zinc finger, DHHC-type containing 11	-0,33	0,01

4888	NPY6R	neuropeptide Y receptor Y6 (pseudogene)	-0,33	0,03
657	BMPRIA	bone morphogenetic protein receptor, type IA; similar to ALK-3	-0,34	0,01
9587	MAD2L1BP	MAD2L1 binding protein	-0,34	0,00
537	ATP6AP1	ATPase, H+ transporting, lysosomal accessory protein 1	-0,34	0,01
10654	PMVK	phosphomevalonate kinase	-0,34	0,00
28955	DEXI	dexamethasone-induced transcript	-0,34	0,00
91380	SNORD107	small nucleolar RNA, C/D box 107	-0,34	0,00
6444	SGCD	sarcoglycan, delta (35kDa dystrophin-associated glycoprotein)	-0,34	0,05
9524	TECR	glycoprotein, synaptic 2	-0,34	0,01
64756	ATPAF1	ATP synthase mitochondrial F1 complex assembly factor 1	-0,34	0,01
5523	PPP2R3A	protein phosphatase 2 (formerly 2A), regulatory subunit B", alpha	-0,34	0,01
1429	CRYZ	crystallin, zeta (quimone reductase)	-0,34	0,01
9249	DHRS3	dehydrogenase/reductase (SDR family) member 3	-0,34	0,00
8082	SSPN	sarcospan (Kras oncogene-associated gene)	-0,34	0,04
2009	EML1	echinoderm microtubule associated protein like 1	-0,34	0,00
9099	USP2	ubiquitin specific peptidase 2	-0,34	0,00
55245	UQCC	ubiquinol-cytochrome c reductase complex chaperone	-0,34	0,01
23433	RHOQ	ras homolog gene family, member Q; similar to small GTP binding protein TC10	-0,34	0,00
4782	NFIC	nuclear factor I/C (CCAAT-binding transcription factor)	-0,34	0,01
9497	SLC4A7	solute carrier family 4, sodium bicarbonate cotransporter, member 7	-0,34	0,03
57493	HEG1	HEG homolog 1 (zebrafish)	-0,34	0,00
284451	ODF3L2	outer dense fiber of sperm tails 3-like 2	-0,34	0,00
5351	PLOD1	procollagen-lysine 1, 2-oxoglutarate 5-dioxygenase 1	-0,35	0,01
84896	ATAD1	ATPase family, AAA domain containing 1	-0,35	0,01
55929	DMAPI	DNA methyltransferase 1 associated protein 1	-0,35	0,01
8854	ALDH1A2	aldehyde dehydrogenase 1 family, member A2	-0,35	0,03
6183	MRPS12	mitochondrial ribosomal protein S12	-0,35	0,00
84681	HINT2	histidine triad nucleotide binding protein 2	-0,35	0,02
11018	TMED1	transmembrane emp24 protein transport domain containing 1	-0,35	0,00
10422	UBAC1	UBA domain containing 1	-0,35	0,00



285440	CYP4V2	cytochrome P450, family 4, subfamily V, polypeptide 2	-0,35	0,00
4240	MFGE8	milk fat globule-EGF factor 8 protein	-0,35	0,00
219348	PLAC9	placenta-specific 9	-0,35	0,03
6453	ITSN1	intersectin 1 (SH3 domain protein)	-0,35	0,00
25842	ASF1A	DKFZP564O0823 protein	-0,35	0,01
151242	PPP1R1C	protein phosphatase 1, regulatory (inhibitor) subunit 1C	-0,35	0,01
81533	ITFG1	integrin alpha FG-GAP repeat containing 1	-0,35	0,01
51085	MLXIPL	MLX interacting protein-like	-0,35	0,00
30011	SH3KBP1	SH3-domain kinase binding protein 1	-0,35	0,01
85457	KIAA1737	KIAA1737	-0,35	0,04
90135	BTBD6	BTB (POZ) domain containing 6	-0,35	0,00
3373	HYAL1	hyaluronoglucosaminidase 1	-0,35	0,01
170302	ARX	aristales related homeobox	-0,36	0,00
29083	GTPBP8	GTP-binding protein 8 (putative)	-0,36	0,01
54345	SOX18	SRY (sex determining region Y)-box 18	-0,36	0,05
55333	SYNJ2BP	synaptotagmin 2 binding protein	-0,36	0,01
23767	FLRT3	fibronectin leucine rich transmembrane protein 3	-0,36	0,01
6253	RTN2	reticulon 2	-0,36	0,05
7423	VEGFB	vascular endothelial growth factor B	-0,36	0,00
2178	FANCE	Fanconi anemia, complementation group E	-0,36	0,00
5104	SERPINA5	serpin peptidase inhibitor, clade A (alpha-1 antiproteinase, antitrypsin), member 5	-0,36	0,01
92241	RCSD1	RCSD domain containing 1	-0,36	0,00
5774	PTPN3	protein tyrosine phosphatase, non-receptor type 3	-0,36	0,03
161247	FIT1	fat storage-inducing transmembrane protein 1	-0,36	0,01
7360	UGP2	UDP-glucose pyrophosphorylase 2	-0,36	0,01
51207	DUSP13	dual specificity phosphatase 13	-0,36	0,01
55625	ZDHC7	zinc finger, DHHC-type containing 7	-0,36	0,00
23646	PLD3	phospholipase D family, member 3	-0,37	0,01
51660	BRP44L	brain protein 44-like	-0,37	0,02
81621	KAZALD1	Kazal-type serine peptidase inhibitor domain 1	-0,37	0,02

<b>6391</b>	SDHC	succinate dehydrogenase complex, subunit C, integral membrane protein, 15kDa	-0,37	0,00
<b>6867</b>	TACC1	transforming, acidic coiled-coil containing protein 1	-0,37	0,02
<b>10572</b>	SIVA	SIVA1, apoptosis-inducing factor	-0,37	0,03
<b>55353</b>	LAPTM4B	lysosomal protein transmembrane 4 beta	-0,37	0,00
<b>2819</b>	GPD1	glycerol-3-phosphate dehydrogenase 1 (soluble)	-0,37	0,05
<b>4700</b>	NDUFA6	NADH dehydrogenase (ubiquinone) 1 alpha subcomplex, 6, 14kDa	-0,37	0,01
<b>8405</b>	SPOP	speckle-type POZ protein	-0,37	0,00
<b>23344</b>	ESYT1	family with sequence similarity 62 (C2 domain containing), member A	-0,37	0,01
<b>8996</b>	NOL3	nucleolar protein 3 (apoptosis repressor with CARD domain)	-0,37	0,01
<b>3270</b>	HRC	histidine rich calcium binding protein	-0,37	0,00
<b>27335</b>	EIF3K	eukaryotic translation initiation factor 3, subunit K	-0,37	0,02
<b>57446</b>	NDRG3	NDRG family member 3	-0,38	0,05
<b>84191</b>	FAM96A	family with sequence similarity 96, member A	-0,38	0,02
<b>114782</b>	KIAA1881	phosphoinositide-3-kinase interacting protein 1	-0,38	0,02
<b>57380</b>	MRS2	MRS2 magnesium homeostasis factor homolog (S. cerevisiae)	-0,38	0,01
<b>53632</b>	PRKAG3	protein kinase, AMP-activated, gamma 3 non-catalytic subunit	-0,38	0,02
<b>815</b>	CAMK2A	calcium/calmodulin-dependent protein kinase II alpha	-0,38	0,02
<b>8483</b>	CILP	cartilage intermediate layer protein, nucleotide pyrophosphohydrolase	-0,38	0,05
<b>284403</b>	WDR62	WD repeat domain 62	-0,38	0,02
<b>2542</b>	SLC37A4	solute carrier family 37 (glucose-6-phosphate transporter), member 4	-0,38	0,01
<b>8728</b>	ADAM19	ADAM metalloproteinase domain 19 (meltrin beta)	-0,38	0,00
<b>51537</b>	MTP18	mitochondrial protein 18 kDa	-0,38	0,00
<b>23240</b>	KIAA0922	KIAA0922	-0,38	0,04
<b>10867</b>	TSPAN9	tetraspanin 9	-0,38	0,00
<b>131474</b>	CHCHD4	coiled-coil-helix-coiled-coil-helix domain containing 4	-0,38	0,00
<b>4702</b>	NDUFA8	NADH dehydrogenase (ubiquinone) 1 alpha subcomplex, 8, 19kDa	-0,39	0,01
<b>339896</b>	GADL1	glutamate decarboxylase-like 1	-0,39	0,02
<b>4239</b>	MFAP4	microfibrillar-associated protein 4	-0,39	0,05
<b>9958</b>	USP15	ubiquitin specific peptidase 15	-0,39	0,02
<b>56910</b>	STARD7	STAR-related lipid transfer (START) domain containing 7	-0,39	0,01

928	CD9	CD9 molecule	-0,39	0,00
27122	DKK3	dickkopf homolog 3 ( <i>Xenopus laevis</i> )	-0,39	0,01
27231	ITGB1BP3	integrin beta 1 binding protein 3	-0,40	0,02
4128	MAOA	monoamine oxidase A	-0,40	0,05
51204	TACO1	coiled-coil domain containing 44	-0,40	0,00
57571	ATPGD1	ATP-grasp domain containing 1	-0,40	0,03
3743	KCNA7	potassium voltage-gated channel, shaker-related subfamily, member 7	-0,40	0,00
64801	ARV1	ARV1 homolog ( <i>S. cerevisiae</i> )	-0,40	0,00
284119	PTRF	polymerase I and transcript release factor	-0,40	0,00
845	CASQ2	calsequestrin 2 (cardiac muscle)	-0,40	0,02
339456	TMEM52	transmembrane protein 52	-0,40	0,03
25849	PARM1	SIN3 homolog A, transcription regulator (yeast)	-0,40	0,00
26273	FBXO3	3-hydroxyisobutyryl-Coenzyme A hydrolase	-0,40	0,03
84281	MGC13057	chromosome 2 open reading frame 88	-0,40	0,00
3052	HCCS	holocytochrome c synthase (cytochrome c heme-lyase)	-0,41	0,00
441531	PGAM4	phosphoglycerate mutase family member 4	-0,41	0,01
5376	PMP22	peripheral myelin protein 22	-0,41	0,03
306	ANXA3	annexin A3	-0,41	0,00
148932	MOBK12C	MOB1, Mps One Binder kinase activator-like 2C (yeast)	-0,41	0,02
3590	IL11RA	interleukin 11 receptor, alpha	-0,42	0,00
29903	CCDC106	coiled-coil domain containing 106	-0,42	0,00
4624	MYH6	myosin, heavy chain 6, cardiac muscle, alpha	-0,42	0,02
23095	KIF1B	kinesin family member 1B	-0,42	0,00
79191	IRX3	iroquois homeobox 3	-0,42	0,04
113457	TUBA3D	tubulin, alpha 3d; tubulin, alpha 3c	-0,42	0,00
94274	PPP1R14A	protein phosphatase 1, regulatory (inhibitor) subunit 14A	-0,42	0,00
130827	TMEM182	transmembrane protein 182	-0,43	0,05
4208	MEF2C	myocyte enhancer factor 2C	-0,43	0,03
29	ABR	active BCR-related gene	-0,43	0,00
9922	IQSEC1	IQ motif and Sec7 domain 1	-0,43	0,00

<b>80206</b>	FHOD3	formin homology 2 domain containing 3	-0,43	0,01
<b>8028</b>	MLLT10	myeloid/lymphoid or mixed-lineage leukemia (trithorax homolog, Drosophila); translocated to, 10	-0,43	0,00
<b>4094</b>	MAF	v-maf musculoaponeurotic fibrosarcoma oncogene homolog (avian)	-0,43	0,00
<b>11155</b>	LDB3	LIM domain binding 3	-0,43	0,01
<b>5588</b>	PRKCQ	protein kinase C, theta	-0,43	0,05
<b>786</b>	CACNG1	calcium channel, voltage-dependent, gamma subunit 1	-0,43	0,00
<b>9719</b>	ADAMTSL2	similar to ADAMTS-like 2; ADAMTS-like 2	-0,43	0,00
<b>2199</b>	FBLN2	fibulin 2	-0,43	0,03
<b>116138</b>	KLHDC3	kelch domain containing 3	-0,44	0,00
<b>26873</b>	OPLAH	HMG-box transcription factor 1	-0,44	0,01
<b>256691</b>	MAMDC2	MAM domain containing 2	-0,44	0,03
<b>2875</b>	GPT	glutamic-pyruvate transaminase (alanine aminotransferase)	-0,44	0,01
<b>253512</b>	SLC25A30	solute carrier family 25, member 30	-0,44	0,00
<b>29796</b>	UCRC	ubiquinol-cytochrome c reductase complex (7.2 kD)	-0,44	0,00
<b>55700</b>	MAP7D1	MAP7 domain containing 1	-0,44	0,00
<b>83543</b>	AIF1L	allograft inflammatory factor 1-like	-0,44	0,03
<b>64328</b>	XPO4	exportin 4	-0,44	0,03
<b>29904</b>	EEF2K	eukaryotic elongation factor-2 kinase	-0,45	0,01
<b>57801</b>	HES4	hairy and enhancer of split 4 (Drosophila)	-0,45	0,00
<b>5287</b>	PIK3C2B	phosphoinositide-3-kinase, class 2, beta polypeptide	-0,45	0,01
<b>284612</b>	SYPL2	synaptophysin-like 2	-0,45	0,01
<b>5961</b>	PRPH2	peripherin 2 (retinal degeneration, slow)	-0,45	0,03
<b>9499</b>	MYOT	myotilin	-0,45	0,00
<b>8195</b>	MKKS	McKusick-Kaufman syndrome	-0,46	0,00
<b>23052</b>	ENDOD1	endonuclease domain containing 1	-0,46	0,00
<b>80772</b>	GLTPDI	glycolipid transfer protein domain containing 1	-0,46	0,00
<b>10039</b>	PARP3	poly (ADP-ribose) polymerase family, member 3	-0,46	0,00
<b>142685</b>	ASB15	ankyrin repeat and SOCS box-containing 15	-0,47	0,01
<b>51805</b>	COQ3	coenzyme Q3 homolog, methyltransferase (S. cerevisiae)	-0,47	0,01

84908	FAM136A	family with sequence similarity 136, member A	-0,47	0,00
64981	MRPL34	mitochondrial ribosomal protein L34	-0,47	0,00
54536	EXOC6	exocyst complex component 6	-0,48	0,01
5150	PDE7A	phosphodiesterase 7A	-0,48	0,00
7871	SLMAP	sarcolemma associated protein	-0,48	0,02
595	CCND1	cyclin D1	-0,48	0,00
91977	MYOZ3	myozenin 3	-0,48	0,00
7283	TUBG1	tubulin, gamma 1; similar to Tubulin, gamma 1	-0,48	0,00
23112	TNRC6B	trinucleotide repeat containing 6B	-0,48	0,00
6790	AURKA	aurora kinase A; aurora kinase A pseudogene 1	-0,48	0,00
10994	ILVBL	ilvB (bacterial acetolactate synthase)-like	-0,48	0,00
11138	TBC1D8	TBC1 domain family, member 8 (with GRAM domain)	-0,49	0,00
245806	VGLL2	vestigial like 2 (Drosophila)	-0,49	0,02
145957	NRG4	neuregulin 4	-0,49	0,00
79140	CCDC28B	coiled-coil domain containing 28B	-0,49	0,00
6821	SUOX	sulfite oxidase	-0,49	0,02
23632	CA14	carbonic anhydrase XIV	-0,49	0,00
3727	JUND	jun D proto-oncogene	-0,50	0,00
84812	PLCD4	phospholipase C, delta 4	-0,50	0,00
84814	PPAPDC3	phosphatidic acid phosphatase type 2 domain containing 3	-0,50	0,02
1737	DLAT	dihydroipoamide S-acetyltransferase	-0,50	0,00
22906	TRAK1	trafficking protein, kinesin binding 1	-0,50	0,00
55234	SMU1	smu-1 suppressor of mec-8 and unc-52 homolog (C. elegans)	-0,50	0,00
178	AGL	amylase-1, 6-glycosidase, 4-alpha-glucanotransferase	-0,50	0,01
6913	TBX15	T-box 15	-0,50	0,00
1634	DCN	decorin	-0,51	0,02
3417	IDH1	isocitrate dehydrogenase 1 (NADP+), soluble	-0,51	0,01
147808	ZNF784	zinc finger protein 784	-0,51	0,00
55334	SLC39A9	solute carrier family 39 (zinc transporter), member 9	-0,51	0,03
3622	ING2	inhibitor of growth family, member 2	-0,51	0,00

27244	SESN1	sestrin 1	-0,51	0,05
7123	CLEC3B	C-type lectin domain family 3, member B	-0,52	0,00
124222	PAQR4	progesterin and adipoQ receptor family member IV	-0,52	0,00
114881	OSBPL7	oxysterol binding protein-like 7	-0,52	0,03
127495	LRRC39	leucine rich repeat containing 39	-0,52	0,02
3422	IDI1	isopentenyl-diphosphate delta isomerase 1	-0,53	0,00
51621	KLF13	Kruppel-like factor 13	-0,53	0,00
84870	RSPO3	R-spondin 3 homolog ( <i>Xenopus laevis</i> )	-0,53	0,02
113655	MFSD3	tubulin, alpha 3d; tubulin, alpha 3c	-0,53	0,00
79365	BHLHB3	basic helix-loop-helix family, member e41	-0,53	0,00
51676	ASB2	ankyrin repeat and SOCS box-containing 2	-0,53	0,00
1628	DBP	D site of albumin promoter (albumin D-box) binding protein	-0,53	0,01
136371	ASB10	ankyrin repeat and SOCS box-containing 10	-0,54	0,00
79594	MUL1	mitochondrial E3 ubiquitin ligase 1	-0,54	0,00
54873	PALMD	palmdelphin	-0,54	0,01
5648	MASPI	mannan-binding lectin serine peptidase 1 (C4/C2 activating component of Ra-reactive factor)	-0,55	0,00
1573	CYP2J2	cytochrome P450, family 2, subfamily J, polypeptide 2	-0,55	0,00
7277	TUBA4A	tubulin, alpha 4a	-0,55	0,00
6512	SLC1A7	solute carrier family 1 (glutamate transporter), member 7	-0,55	0,00
80303	EFHD1	EF-hand domain family, member D1	-0,55	0,01
25780	RASGRP3	beta-site APP-cleaving enzyme 2	-0,55	0,01
286101	ZNF252	zinc finger protein 252	-0,56	0,00
3177	SLC29A2	solute carrier family 29 (nucleoside transporters), member 2	-0,56	0,04
1649	DDIT3	DNA-damage-inducible transcript 3	-0,56	0,00
6275	S100A4	S100 calcium binding protein A4	-0,57	0,02
150572	SMYD1	SET and MYND domain containing 1	-0,57	0,00
165186	FAM179A	family with sequence similarity 179, member A	-0,57	0,02
23066	CAND2	cullin-associated and neddylation-dissociated 2 (putative)	-0,57	0,00
126755	LRRC38	leucine rich repeat containing 38	-0,57	0,01

4330	MN1	meningioma (disrupted in balanced translocation) 1	-0,58	0,03
51449	PCYOX1	prenyllysine oxidase 1	-0,59	0,01
57644	MYH7B	myosin, heavy chain 7B, cardiac muscle, beta	-0,59	0,00
1396	CRIP1	cysteine-rich protein 1 (intestinal)	-0,59	0,00
7422	VEGFA	vascular endothelial growth factor A	-0,60	0,00
57142	RTN4	reticulon 4	-0,60	0,01
79933	SYNPO2L	synaptopodin 2-like	-0,60	0,01
79929	MAP6D1	MAP6 domain containing 1	-0,60	0,00
137735	ABRA	actin-binding Rho activating protein	-0,60	0,05
5959	RDH5	retinol dehydrogenase 5 (11-cis/9-cis)	-0,61	0,00
51318	MRPL35	mitochondrial ribosomal protein L35	-0,61	0,00
6525	SMTN	smoothelin	-0,62	0,00
284	ANGPT1	angiopoietin 1	-0,63	0,01
221662	RBM24	RNA binding motif protein 24	-0,63	0,03
361	AQP4	aquaporin 4	-0,63	0,04
85366	MYLK2	myosin light chain kinase 2	-0,63	0,02
57467	HHATL	hedgehog acyltransferase-like	-0,64	0,00
54463	FAM134B	family with sequence similarity 134, member B	-0,64	0,03
26027	ACOT11	WD repeat domain 21A	-0,64	0,00
43	ACHE	acetylcholinesterase (Yt blood group)	-0,66	0,00
1490	CTGF	connective tissue growth factor	-0,66	0,02
51285	RASL12	RAS-like, family 12	-0,67	0,00
64682	ANAPC1	anaphase promoting complex subunit 1; similar to anaphase promoting complex subunit 1	-0,68	0,00
122416	ANKRD9	ankyrin repeat domain 9	-0,68	0,00
53354	PANK1	pantothenate kinase 1	-0,68	0,00
160760	PPTC7	PTC7 protein phosphatase homolog (S. cerevisiae)	-0,71	0,00
9935	MAFB	v-maf musculoaponeurotic fibrosarcoma oncogene homolog B (avian)	-0,71	0,00
91663	MYADM	myeloid-associated differentiation marker	-0,71	0,00
93058	COQ10A	coenzyme Q10 homolog A (S. cerevisiae)	-0,71	0,00
3306	HSPA2	heat shock 70kDa protein 2	-0,72	0,00

4060	LUM	lumican	-0,72	0,00
53342	IL17D	interleukin 17D	-0,75	0,02
286	ANK1	ankyrin 1, erythrocytic	-0,75	0,00
64793	CCDC21	coiled-coil domain containing 21	-0,77	0,00
14	AAMP	angio-associated, migratory cell protein	-0,78	0,00
284358	FLJ36070	MEF2 activating motif and SAP domain containing transcriptional regulator	-0,78	0,01
340156	MYLK4	myosin light chain kinase family, member 4	-0,80	0,00
23439	ATP1B4	ATPase, (Na <sup>+</sup> )/K <sup>+</sup> transporting, beta 4 polypeptide	-0,80	0,01
5506	PPP1R3A	protein phosphatase 1, regulatory (inhibitor) subunit 3A	-0,85	0,00
84988	PPP1R16A	protein phosphatase 1, regulatory (inhibitor) subunit 16A	-0,86	0,00
79156	PLEKHF1	pleckstrin homology domain containing, family F (with FYVE domain) member 1	-0,91	0,00
10140	TOB1	transducer of ERBB2, 1	-1,00	0,00
5507	PPP1R3C	protein phosphatase 1, regulatory (inhibitor) subunit 3C	-1,01	0,00
123722	FSD2	fibronectin type III and SPRY domain containing 2	-1,05	0,00
10891	PPARGC1A	peroxisome proliferator-activated receptor gamma, coactivator 1 alpha	-1,10	0,00
6876	TAGLN	transgelin	-1,10	0,00
50486	G0S2	G0/G1 switch 2	-1,14	0,01
388228	SBK1	SH3-binding domain kinase 1	-1,17	0,00
9123	SLC16A3	solute carrier family 16, member 3 (monocarboxylic acid transporter 4)	-1,32	0,00
59	ACTA2	actin, alpha 2, smooth muscle, aorta	-1,50	0,00
7037	TFRC	transferrin receptor (p90, CD71)	-1,53	0,00
114789	SLC25A25	solute carrier family 25 (mitochondrial carrier; phosphate carrier), member 25	-1,64	0,00



